bioRxiv preprint doi: https://doi.org/10.1101/041509; this version posted February 26, 2016. The copyright holder for this preprint (which was not certified by peer review) is the author/funder. All rights reserved. No reuse allowed without permission.

How domain growth is implemented determines the long term behaviour of a cell population through its effect on spatial correlations.

Robert J. H. Ross *[1], R. E. Baker †[1], and C. A. Yates ‡[2]

[1]Wolfson Centre for Mathematical Biology, Mathematical Institute, University of Oxford, Radcliffe Observatory Quarter, Woodstock Road, Oxford, OX2 6GG

[2]Centre for Mathematical Biology, Department of Mathematical Sciences, University of Bath, Claverton Down, Bath, BA2 7AY

February 24, 2016

Abstract

Domain growth plays an important role in many biological systems, and so the inclusion of domain growth in models of these biological systems is important to understanding how these biological systems function. In this work we present methods to include the effects of domain growth on the evolution of spatial correlations in a continuum approximation of a lattice-based model of cell motility and proliferation. We show that, depending on the way in which domain growth is implemented, different steady-state densities are predicted for an agent population. Furthermore, we demonstrate that the way in which domain growth is implemented can result in the evolution of the agent density depending on the size of the domain. Continuum approximations that ignore spatial correlations cannot capture these behaviours, while those that account for spatial correlations do. These results will be of interest to researchers in developmental biology, as they suggest that the nature of domain growth can determine the characteristics of cell populations.

*ross@maths.ox.ac.uk
†baker@maths.ox.ac.uk
‡c.yates@bath.ac.uk

bioRxiv preprint doi: https://doi.org/10.1101/041509; this version posted February 26, 2016. The copyright holder for this preprint (which was not certified by peer review) is the author/funder. All rights reserved. No reuse allowed without permission.

1 Introduction

Growth is of fundamental importance in biological systems [1, 2]. From embryonic development to tissue renewal, growth plays a central role in the development, maintenance and repair of biological systems throughout their lifetime [3]. Types of isotropic growth that have been observed in biological systems include exponential, linear and logistic [4–11]. Anisotropic growth also plays an important role in biological systems. For instance apical growth, whereby the tip region of a domain grows, is observed in plant root extension and chick limb outgrowth [12, 13]. Importantly, growth has also been shown to contribute in the development of biological systems in different ways. Experiments have shown that the advective component of domain growth is important in enabling migrating cells to reach their target site [6–9]. Meanwhile, theoretical studies have suggested that differential growth rates in developing tissue allow the generation of diverse biological forms and structures [10, 14]. Consequently, it is important to include domain growth in many models of biological systems [1, 2, 6–9, 14–18].

Spatial correlations are often observed in biological systems [19–24]. For instance, in cell populations spatial correlations can be established by cell proliferation, as a new cell is naturally close to its parent cell following division. Individual-based models (IBMs) are able to recapitulate these spatial correlations, whereas models that employ certain mean-field approximations (MFAs), such as the logistic model [25], and, in a spatially-extended context, the diffusion equation, cannot [26–30]. Accurate continuum models are important tools for understanding the behaviour of biological systems as, in contrast to IBMs, they generally allow for greater mathematical analysis. This analysis can be crucial in forming a mechanistic understanding of biological systems, which is not always apparent from simply studying the results of a large number of repeats of an IBM. Therefore, in order to derive accurate continuum approximations of IBMs that include cell proliferation it is often necessary to account for the effects of spatial correlations [25, 31–39].

In this work we examine how domain growth affects the evolution of spatial correlations between agents in IBMs, and importantly, how the way in which domain growth is implemented affects spatial correlations differently. To do so we use an agent-based (our agents represent

bioRxiv preprint doi: https://doi.org/10.1101/041509; this version posted February 26, 2016. The copyright holder for this preprint (which was not certified by peer review) is the author/funder. All rights reserved. No reuse allowed without permission.

cells), discrete random-walk model on a two-dimensional square lattice with volume-exclusion. We had reasoned that a standard MFA would not be able to capture the behaviours exhibited by the IBM, and that this standard MFA would require correction by the inclusion of spatial correlations in the form of a correlation ordinary differential equation (ODE) to accurately approximate the IBM results. This last point has been shown previously in scenarios without growth [25].

The outline of this work is as follows: to begin with we introduce the IBM and growth mechanisms in Section 2.1. We then define our individual and pairwise density functions, and derive a system of ODEs describing the evolution of the individual and pairwise density functions with respect to time on a growing domain in Sections 2.2-2.3. To test the accuracy of these ODE models we compare them with ensemble averages for the evolution of the macroscopic density from the IBM in Section 3. We demonstrate that the standard MFA is not able to accurately capture the effects of domain growth in the IBM, whereas the ODE models that include the effect of spatial correlations do.

2 Model

In this section we introduce the IBM and the domain growth mechanisms we employ throughout this work. We then derive equations describing the evolution of the individual and pairwise density functions in the IBM for both growth mechanisms.

2.1 IBM and domain growth mechanisms

Our two-dimensional square lattice has lattice spacing Δ [40] and size $N_x(t)$ by $N_y(t)$, where $N_x(t)$ is the number of lattice sites in a row and $N_y(t)$ is the number of sites in a column. This type of model has been used frequently to model biological processes [10, 21, 41, 42]. All simulations are performed with periodic boundary conditions, and throughout this work the lattice spacing, Δ, is equal to one. For notational convenience we shall now write $N_x(t)$ as N_x, and $N_y(t)$ as N_y.

In the IBM each agent is initially assigned to a lattice site, from which it can move or pro-

bioRxiv preprint doi: https://doi.org/10.1101/041509; this version posted February 26, 2016. The copyright holder for this preprint (which was not certified by peer review) is the author/funder. All rights reserved. No reuse allowed without permission.

liferate into an adjacent site. If an agent attempts to move into a site that is already occupied, the movement event is aborted. Similarly, if an agent attempts to proliferate into a site that is already occupied, the proliferation event is aborted. This process, whereby only one agent is allowed per site, is generally referred to as an exclusion process [40]. Time is evolved continuously, in accordance with the Gillespie algorithm [43], such that movement, proliferation and growth events are modelled as exponentially distributed 'reaction events' in a Markov chain. Attempted agent movement or proliferation events occur with rates P_m or P_p per unit time, respectively. For example, $P_m \delta t$ is the probability of an agent attempting to move in the next infinitesimally small time interval δt. Throughout this work the initial agent distribution for all simulations of the IBM is achieved by populating lattice sites uniformly at random until the required density is achieved.

Both growth mechanisms we employ are stochastic growth mechanisms [10]: the insertion of new lattice sites into the domain occurs with positive rate constants P_{g_x} and P_{g_y} per unit time, for growth in the x (horizontal) and y (vertical) directions, respectively. That is, each lattice site undergoes a growth event in the x direction with rate P_{g_x}. This means the total rate of domain growth in the x direction is $P_{g_x} N_x$. In growth mechanism 1 (GM1) when a 'growth event' occurs along the x axis (horizontal axis in Fig. 1), one new column of sites is added at a position selected uniformly at random. In growth mechanism 2 (GM2) when a 'growth event' occurs along the x axis (horizontal axis in Fig. 1), for each row, one new site is added in a column which is selected uniformly at random. Importantly, when a growth event occurs, the site selected for division is moved one spacing in the positive horizontal/vertical direction along with its contents (i.e. an agent or no agent, symbolised by a black circle in Fig. 1). The new lattice site is empty, and the contents of all other lattice sites remain unaffected. Growth in the y direction is implemented in an analogous manner to the x direction for both growth mechanisms. We chose these growth mechanisms as they are significantly different to each other, and both may have biological relevance [44–46]. For example, biological growth similar to GM1 can occur when adjacent cells become synchronous in their cell cycles (that is, the underlying cells that form the domain). Furthermore, both of these growth mechanisms can be used to implement any form of isotropic growth in our IBM, and are adaptable to three spatial

bioRxiv preprint doi: https://doi.org/10.1101/041509; this version posted February 26, 2016. The copyright holder for this preprint (which was not certified by peer review) is the author/funder. All rights reserved. No reuse allowed without permission.

dimensions [10]. Finally, it is important to stress that both growth mechanisms give rise to the same overall growth rate when implemented with the same growth rate parameters.

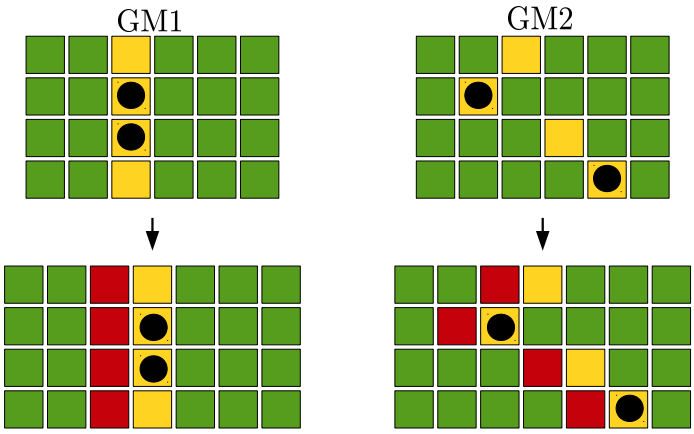

Figure 1: (Colour online). Before and after the growth events for both GM1 and GM2, in which growth is along the x-axis (horizontal direction) for a two-dimensional lattice. In each row the yellow (light grey) site has been chosen to undergo a growth event. Following this the yellow (light grey) site is moved to the right with its contents, for instance an agent (represented by a black cell). The red (dark grey) sites are the new lattice sites and are always initially empty. The contents of all the other sites remain unaffected, although in some cases their neighbouring sites will change.

2.2 Individual density functions

We define $\rho_1^{N_x \times N_y}(\mathbf{m}; t)$ as the probability that site $\mathbf{m}$ is occupied by an agent at time t on a domain of size $N_x \times N_y$, where $\mathbf{m}$ is the vector (i, j), with i indexing the row number of a lattice site, and j indexing the column number of a lattice site. For instance, $(2, 3)$ would be the lattice site situated in the second row and the third column of the lattice.

The following derivation for the individual density functions is the same for GM1 and GM2.

bioRxiv preprint doi: https://doi.org/10.1101/041509; this version posted February 26, 2016. The copyright holder for this preprint (which was not certified by peer review) is the author/funder. All rights reserved. No reuse allowed without permission.

The sum of the individual density functions on a domain of size $N_x \times N_y$ at $[t+\delta t)$ is such that

$$\begin{aligned}\sum_{i=1}^{N_x}\sum_{j=1}^{N_y}\rho_1^{N_x\times N_y}(\mathbf{m};t+\delta t) &= (1-\delta t P_{g_x}N_x-\delta t P_{g_y}N_y)\sum_{i=1}^{N_x}\sum_{j=1}^{N_y}\rho_1^{N_x\times N_y}(\mathbf{m};t)\\ &+\delta t P_{g_x}\sum_{i=1}^{N_x-1}\sum_{j=1}^{N_y}(N_x-1)\rho_1^{(N_x-1)\times N_y}(\mathbf{m};t)\\ &+\delta t P_{g_y}\sum_{i=1}^{N_x}\sum_{j=1}^{N_y-1}(N_y-1)\rho_1^{N_x\times(N_y-1)}(\mathbf{m};t)+\mathcal{O}(\delta t^2). \qquad (1)\end{aligned}$$

The terms on the RHS of Eq. (1) correspond to the following events: i) the sum of individual density functions on a domain of size $N_x \times N_y$ at time t multiplied by the probability that no growth event occurs in $[t, t+\delta t)$; ii) the sum of individual density functions on a domain of size $(N_x-1)\times N_y$ at time t multiplied by the probability that a growth event occurs in the horizontal (x) direction in $[t, t+\delta t)$; and iii) the sum of individual density functions on a domain of size $N_x \times (N_y-1)$ at time t multiplied by the probability that a growth event occurs in the vertical (y) direction in $[t, t+\delta t)$. Due to our initial conditions in the IBM we can assume translational invariance for the probability of an agent occupying a site in this derivation, by this we mean

$$\rho_1^{N_x\times N_y}(\mathbf{m};t)=\rho_1^{N_x\times N_y}(\mathbf{n};t), \quad \forall \mathbf{m},\mathbf{n}, \qquad (2)$$

where $\mathbf{n}$ indexes any other site on the domain.[1] Therefore we can rewrite Eq. (1) as

$$\begin{aligned}(N_x)(N_y)\rho_1^{N_x\times N_y}(\mathbf{m};t+\delta t) &= (1-\delta t P_{g_x}N_x-\delta t P_{g_y}N_y)(N_x)(N_y)\rho_1^{N_x\times N_y}(\mathbf{m};t)\\ &+\delta t P_{g_x}(N_x-1)(N_y)(N_x-1)\rho_1^{(N_x-1)\times N_y}(\mathbf{m};t)\\ &+\delta t P_{g_y}(N_x)(N_y-1)(N_y-1)\rho_1^{N_x\times(N_y-1)}(\mathbf{m};t)+\mathcal{O}(\delta t^2). \qquad (3)\end{aligned}$$

[1] We can assume translational invariance throughout this work because the initial agent density for all simulations in the IBM are achieved by populating lattice sites uniformly at random until the required density is achieved.

bioRxiv preprint doi: https://doi.org/10.1101/041509; this version posted February 26, 2016. The copyright holder for this preprint (which was not certified by peer review) is the author/funder. All rights reserved. No reuse allowed without permission.

We can simplify Eq. (3) in the following manner

$$\begin{aligned}\rho_1^{N_x\times N_y}(\mathbf{m};t+\delta t) &= (1-\delta t P_{g_x}N_x - \delta t P_{g_y}N_y)\rho_1^{N_x\times N_y}(\mathbf{m};t)\\ &+ \delta t P_{g_x}\left(\frac{N_x-1}{N_x}\right)(N_x-1)\rho_1^{(N_x-1)\times N_y}(\mathbf{m};t)\\ &+ \delta t P_{g_y}\left(\frac{N_y-1}{N_y}\right)(N_y-1)\rho_1^{N_x\times(N_y-1)}(\mathbf{m};t) + \mathcal{O}(\delta t^2). \qquad (4)\end{aligned}$$

If we now rearrange Eq. (4) and take the limit as $\delta t \to 0$ we obtain

$$\begin{aligned}\frac{\mathrm{d}\rho_1^{N_x\times N_y}(\mathbf{m};t)}{\mathrm{d}t} &= -(P_{g_x}N_x + P_{g_y}N_y)\rho_1^{N_x\times N_y}(\mathbf{m};t)\\ &+ P_{g_x}\left(\frac{N_x-1}{N_x}\right)(N_x-1)\rho_1^{(N_x-1)\times N_y}(\mathbf{m};t)\\ &+ P_{g_y}\left(\frac{N_y-1}{N_y}\right)(N_y-1)\rho_1^{N_x\times(N_y-1)}(\mathbf{m};t). \qquad (5)\end{aligned}$$

If we make the approximation $\rho_1^{N_x\times N_y}(\mathbf{m};t) \approx ((N_y-1)/N_y)\,\rho_1^{N_x\times(N_y-1)}(\mathbf{m};t)$ and $\rho_1^{N_x\times N_y}(\mathbf{m};t) \approx ((N_x-1)/N_x)\,\rho_1^{(N_x-1)\times N_y}(\mathbf{m};t)$, Eq. (5) can be written as

$$\begin{aligned}\frac{\mathrm{d}\rho_1^{N_x\times N_y}(\mathbf{m};t)}{\mathrm{d}t} &= -(P_{g_x}N_x + P_{g_y}N_y)\rho_1^{N_x\times N_y}(\mathbf{m};t)\\ &+ P_{g_x}(N_x-1)\rho_1^{N_x\times N_y}(\mathbf{m};t)\\ &+ P_{g_y}(N_y-1)\rho_1^{N_x\times N_y}(\mathbf{m};t). \qquad (6)\end{aligned}$$

This approximation has been previously published [17], and implies that domain growth 'dilutes' the agent density. Finally, we simplify Eq. (6) to obtain

$$\frac{\mathrm{d}\rho_1^{N_x\times N_y}(\mathbf{m};t)}{\mathrm{d}t} = -(P_{g_x}+P_{g_y})\rho_1^{N_x\times N_y}(\mathbf{m};t). \qquad (7)$$

Eq. (7) describes how exponential domain growth affects agent density. As we will write the pairwise density functions in terms of the distances between sites, we shall rewrite the individual density functions as

$$\rho_1^{N_x\times N_y}(\mathbf{m};t) = c(t). \qquad (8)$$

bioRxiv preprint doi: https://doi.org/10.1101/041509; this version posted February 26, 2016. The copyright holder for this preprint (which was not certified by peer review) is the author/funder. All rights reserved. No reuse allowed without permission.

If we substitute Eq. (8) into Eq. (7) we obtain

$$\frac{\mathrm{d}c(t)}{\mathrm{d}t} = -(P_{g_x} + P_{g_y})c(t). \tag{9}$$

Eq. (9) is a MFA describing the effect of domain growth on the evolution agent density [32].

2.3 Pairwise density functions

We now derive the terms necessary to include the effect of two-dimensional exponential domain growth in the evolution of the pairwise density functions. Importantly, GM1 and GM2 affect the evolution of the pairwise density functions differently. Figure 2 displays two configurations of two agents, which we will term colinear and diagonal.

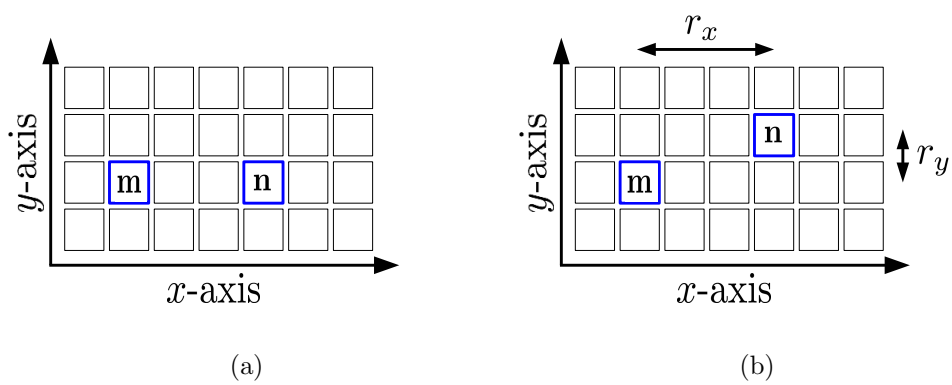

Figure 2: The two types of configuration of lattice sites: (a) colinear and (b) diagonal. The lattice sites in question are labelled **m** and **n** and bordered by blue. In (a), two colinear lattice sites share the same row but not the same column (or vice versa). In (b), two lattice sites are diagonal, meaning they do not share the same row or column. r_x is the distance between two lattice sites in the horizontal direction, r_y is the distance between two lattice sites in the vertical direction. In (b) this means $r_x = 3$ and $r_y = 1$.

The horizontal and vertical distances between sites is measured from their centres as displayed in Fig. 2 (b), and r_x is the distance between two lattice sites in the horizontal direction, r_y is the distance between two lattice sites in the vertical direction.

2.3.1 GM1

We define the pairwise density functions, $\rho_2^{N_x \times N_y}(\mathbf{m}, \mathbf{n}; t)$, as the probability sites **m** and **n** are occupied at time t on a domain of size $N_x \times N_y$ (where $\mathbf{m} \neq \mathbf{n}$). We now rewrite $\rho_2^{N_x \times N_y}(\mathbf{m}, \mathbf{n}; t)$

bioRxiv preprint doi: https://doi.org/10.1101/041509; this version posted February 26, 2016. The copyright holder for this preprint (which was not certified by peer review) is the author/funder. All rights reserved. No reuse allowed without permission.

in terms of the distance between lattice sites, that is

$$\rho_2^{N_x \times N_y}(\mathbf{m}, \mathbf{n}; t) = \rho_2^{N_x \times N_y}(\mathbf{m}, \mathbf{m} + (r_x, r_y); t), \tag{10}$$

where $\mathbf{m}$ is (i, j), with i indexing the row number of a lattice site, j indexing the column number of a lattice site, and (r_x, r_y) is a vector that represents a fixed displacement as defined in Fig. 2.

Due to the initial conditions of the IBM we are able to assume translational invariance for the probability of two sites a given distance being occupied, which means the pairwise density function can be written as a function of the distance between two lattice sites, (r_x, r_y). Therefore, we will further simplify our notation to obtain

$$\rho_2^{N_x \times N_y}(\mathbf{m}, \mathbf{m} + (r_x, r_y); t) = \rho_2^{N_x \times N_y}(r_x, r_y; t). \tag{11}$$

This 'abuse' of notation, whereby ρ_2^L is rewritten as a function of the distance between two lattice sites as opposed to the lattice sites themselves, will prove useful in the following derivation.

Colinear component

For agents colinear in the horizontal direction, that is, $r_y = 0$, the evolution of the pairwise density functions for GM1 is

$$\begin{aligned}
\sum_{i=1}^{N_x}\sum_{j=1}^{N_y} \rho_2^{N_x \times N_y}(r_x, 0; t + \delta t) = {} & (1 - \delta t P_{g_x} N_x - \delta t P_{g_y} N_y) \sum_{i=1}^{N_x}\sum_{j=1}^{N_y} \rho_2^{N_x \times N_y}(r_x, 0; t) \\
& + \delta t P_{g_x} \sum_{i=1}^{N_x - 1}\sum_{j=1}^{N_y} (r_x - 1)\rho_2^{(N_x - 1) \times N_y}(r_x - 1, 0; t) \\
& + \delta t P_{g_x} \sum_{i=1}^{N_x - 1}\sum_{j=1}^{N_y} (N_x - 1 - r_x)\rho_2^{(N_x - 1) \times N_y}(r_x, 0; t) \\
& + \delta t P_{g_y} \sum_{i=1}^{N_x}\sum_{j=1}^{N_y - 1} (N_y - 1)\rho_2^{N_x \times (N_y - 1)}(r_x, 0; t) + \mathcal{O}(\delta t^2).
\end{aligned} \tag{12}$$

The terms on the RHS represent: i) the sum of pairwise density functions for a distance $(r_x, 0)$ apart on a domain of size $N_x \times N_y$ multiplied by the probability that no growth event occurs

bioRxiv preprint doi: https://doi.org/10.1101/041509; this version posted February 26, 2016. The copyright holder for this preprint (which was not certified by peer review) is the author/funder. All rights reserved. No reuse allowed without permission.

in $[t, t+\delta t)$; ii) the sum of pairwise density functions a distance $(r_x - 1, 0)$ apart on a domain of size $(N_x - 1) \times N_y$ at time t multiplied by the probability that a growth event occurs in the horizontal direction in between them moving them $(r_x, 0)$ apart on a domain of size $N_x \times N_y$ at $[t + \delta t)$; iii) the sum of pairwise density functions a distance $(r_x, 0)$ apart on a domain of size $(N_x - 1) \times N_y$ at time t multiplied by the probability that a growth event occurs in the horizontal direction that does not occur between them, meaning that they remain a distance $(r_x, 0)$ apart and on a domain of size $N_x \times N_y$ at time $[t+\delta t)$; and iv) the sum of pairwise density functions a distance $(r_x, 0)$ apart on a domain of size $N_x \times (N_y - 1)$ at time t multiplied by the probability that a growth event occurs in the vertical direction (as the sites are horizontally colinear in this cannot change the distance between them).

Similarly, the evolution of the colinear component for GM1 for agents colinear in the vertical direction, that is, $r_x = 0$, is

$$\begin{aligned}\sum_{i=1}^{N_x}\sum_{j=1}^{N_y}\rho_2^{N_x\times N_y}(0, r_y; t+\delta t) = (1 - \delta t P_{g_x} N_x - \delta t P_{g_y} N_y)\sum_{i=1}^{N_x}\sum_{j=1}^{N_y}\rho_2^{N_x\times N_y}(0, r_y; t) \\ + \delta t P_{g_y}\sum_{i=1}^{N_x}\sum_{j=1}^{N_y-1}(r_y - 1)\rho_2^{N_x\times(N_y-1)}(0, r_y - 1; t) \\ + \delta t P_{g_y}\sum_{i=1}^{N_x}\sum_{j=1}^{N_y-1}(N_y - 1 - r_y)\rho_2^{N_x\times(N_y-1)}(0, r_y; t) \\ + \delta t P_{g_x}\sum_{i=1}^{N_x-1}\sum_{j=1}^{N_y}(N_x - 1)\rho_2^{(N_x-1)\times N_y}(0, r_y; t) + \mathcal{O}(\delta t^2). \qquad (13)\end{aligned}$$

As we assume translational invariance in this derivation, we can simplify Eq. (12) to obtain

$$\begin{aligned}(N_x \times N_y)\rho_2^{N_x\times N_y}(r_x, 0; t+\delta t) = (1 - \delta t P_{g_x} N_x - \delta t P_{g_y} N_y)((N_x \times N_y))\rho_2^{N_x\times N_y}(r_x, 0; t) \\ + \delta t P_{g_x}(((N_x - 1)\times N_y))(r_x - 1)\rho_2^{(N_x-1)\times N_y}(r_x - 1, 0; t) \\ + \delta t P_{g_x}(((N_x - 1)\times N_y))(N_x - 1 - r_x)\rho_2^{(N_x-1)\times N_y}(r_x, 0; t) \\ + \delta t P_{g_y}((N_x \times (N_y - 1)))(N_y - 1)\rho_2^{N_x\times(N_y-1)}(r_x, 0; t) + \mathcal{O}(\delta t^2). \qquad (14)\end{aligned}$$

bioRxiv preprint doi: https://doi.org/10.1101/041509; this version posted February 26, 2016. The copyright holder for this preprint (which was not certified by peer review) is the author/funder. All rights reserved. No reuse allowed without permission.

We can further simplify Eq. (14) to obtain

$$\begin{aligned}\rho_2^{N_x\times N_y}(r_x,0;t+\delta t) = &(1-\delta t P_{g_x}N_x - \delta t P_{g_y}N_y)\rho_2^{N_x\times N_y}(r_x,0;t)\\ &+\delta t P_{g_x}\left(\frac{N_x-1}{N_x}\right)(r_x-1)\rho_2^{(N_x-1)\times N_y}(r_x-1,0;t)\\ &+\delta t P_{g_x}\left(\frac{N_x-1}{N_x}\right)(N_x-1-r_x)\rho_2^{(N_x-1)\times N_y}(r_x,0;t)\\ &+\delta t P_{g_y}\left(\frac{N_y-1}{N_y}\right)(N_y-1)\rho_2^{N_x\times(N_y-1)}(r_x,0;t)+\mathcal{O}(\delta t^2). \qquad (15)\end{aligned}$$

If we apply the approximations $((N_x-1)/N_x)\rho_2^{(N_x-1)\times N_y} \approx \rho_2^{N_x\times N_y}$ and $((N_y-1)/N_y)\rho_2^{N_x\times(N_y-1)} \approx \rho_2^{N_x\times N_y}$, Eq. (15) can be rewritten as

$$\begin{aligned}\rho_2^{N_x\times N_y}(r_x,0;t+\delta t) = &(1-\delta t P_{g_x}N_x - \delta t P_{g_y}N_y)\rho_2^{N_x\times N_y}(r_x,0;t)\\ &+\delta t P_{g_x}(r_x-1)\rho_2^{N_x\times N_y}(r_x-1,0;t)\\ &+\delta t P_{g_x}(N_x-1-r_x)\rho_2^{N_x\times N_y}(r_x,0;t)\\ &+\delta t P_{g_y}(N_y-1)\rho_2^{N_x\times N_y}(r_x,0;t)+\mathcal{O}(\delta t^2). \qquad (16)\end{aligned}$$

If we rearrange Eq. (16) and take the limit as $\delta t \to 0$ we obtain

$$\begin{aligned}\frac{\mathrm{d}\rho_2^{N_x\times N_y}(r_x,0;t)}{\mathrm{d}t} = &P_{g_x}(r_x-1)\rho_2^{N_x\times N_y}(r_x-1,0;t)\\ &-P_{g_x}(r_x+1)\rho_2^{N_x\times N_y}(r_x,0;t)\\ &-P_{g_y}\rho_2^{N_x\times N_y}(r_x,0;t). \qquad (17)\end{aligned}$$

The equivalent equation for sites colinear in the vertical direction is

$$\begin{aligned}\frac{\mathrm{d}\rho_2^{N_x\times N_y}(0,r_y;t)}{\mathrm{d}t} = &P_{g_y}(r_y-1)\rho_2^{N_x\times N_y}(0,r_y-1;t)\\ &-P_{g_y}(r_y+1)\rho_2^{N_x\times N_y}(0,r_y;t)\\ &-P_{g_x}\rho_2^{N_x\times N_y}(0,r_y;t). \qquad (18)\end{aligned}$$

bioRxiv preprint doi: https://doi.org/10.1101/041509; this version posted February 26, 2016. The copyright holder for this preprint (which was not certified by peer review) is the author/funder. All rights reserved. No reuse allowed without permission.

Diagonal component

For the diagonal component for GM1, that is, neither r_x or r_y equal zero, we have

$$\begin{aligned}\sum_{i=1}^{N_x}\sum_{j=1}^{N_y}\rho_2^{N_x\times N_y}(r_x,r_y;t+\delta t) &= (1-\delta t P_{g_x}N_x-\delta t P_{g_y}N_y)\sum_{i=1}^{N_x}\sum_{j=1}^{N_y}\rho_2^{N_x\times N_y}(r_x,r_y;t)\\ &+\delta t P_{g_x}\sum_{i=1}^{N_x-1}\sum_{j=1}^{N_y}(r_x-1)\rho_2^{(N_x-1)\times N_y}(r_x-1,r_y;t)\\ &+\delta t P_{g_x}\sum_{i=1}^{N_x-1}\sum_{j=1}^{N_y}(N_x-1-r_x)\rho_2^{(N_x-1)\times N_y}(r_x,r_y;t)\\ &+\delta t P_{g_y}\sum_{i=1}^{N_x}\sum_{j=1}^{N_y-1}(r_y-1)\rho_2^{N_x\times(N_y-1)}(r_x,r_y-1;t)\\ &+\delta t P_{g_y}\sum_{i=1}^{N_x}\sum_{j=1}^{N_y-1}(N_y-1-r_y)\rho_2^{N_x\times(N_y-1)}(r_x,r_y;t). \qquad (19)\end{aligned}$$

If we follow the same procedure as for the colinear component from Eq. (19) we obtain

$$\begin{aligned}\frac{\mathrm{d}\rho_2^{N_x\times N_y}(r_x,r_y;t)}{\mathrm{d}t} &= P_{g_x}(r_x-1)\rho_2^{N_x\times N_y}(r_x-1,r_y;t)\\ &-P_{g_x}(r_x+1)\rho_2^{N_x\times N_y}(r_x,r_y;t)\\ &+P_{g_y}(r_y-1)\rho_2^{N_x\times N_y-}(r_x,r_y-1;t)\\ &-P_{g_y}(r_y+1)\rho_2^{N_x\times N_y}(r_x,r_y;t). \qquad (20)\end{aligned}$$

For the derivation of the evolution of the pairwise density functions with GM2 we refer the reader to Appendix A. The equation for the colinear component (horizontally colinear) for GM2 is

$$\begin{aligned}\frac{\mathrm{d}\rho_2^{N_x\times N_y}(r_x,0;t)}{\mathrm{d}t} &= -P_{g_x}(r_x+1)\rho_2^{N_x\times N_y}(r_x,0;t)\\ &+P_{g_x}(r_x-1)\rho_2^{N_x\times N_y}(r_x-1,0;t)\\ &+P_{g_y}\left(-1-\frac{N_y}{3}+\frac{1}{3N_y}\right)\rho_2^{N_x\times N_y}(r_x,0;t)\\ &+P_{g_y}\left(-1+\frac{N_y}{3}+\frac{2}{3N_y}\right)\rho_2^{N_x\times N_y}(r_x,-1;t). \qquad (21)\end{aligned}$$

bioRxiv preprint doi: https://doi.org/10.1101/041509; this version posted February 26, 2016. The copyright holder for this preprint (which was not certified by peer review) is the author/funder. All rights reserved. No reuse allowed without permission.

and for the diagonal component in GM2 is

$$\begin{aligned}\frac{\mathrm{d}\rho_2^{N_x\times N_y}(r_x,r_y;t+\delta t)}{\mathrm{d}t} &= P_{g_x}\left(-1-\frac{N_x}{3}+r_x\left(\frac{r_x}{N_x}-1\right)+\frac{1}{3N_x}\right)\rho_2^{N_x\times N_y}(r_x,r_y;t)\\ &+P_{g_y}\left(-1-\frac{N_y}{3}+r_y\left(\frac{r_y}{N_y}-1\right)+\frac{1}{3N_y}\right)\rho_2^{N_x\times N_y}(r_x,r_y;t)\\ &+P_{g_y}\left(-\frac{1}{2}+\frac{N_y}{6}-\frac{r_y}{2}\left(\frac{r_y}{N_y}-1\right)-\frac{1}{3N_y}\right)\rho_2^{N_x\times N_y}(r_x,r_y-1;t)\\ &+P_{g_y}\left(-\frac{1}{2}+\frac{N_y}{6}-\frac{r_y}{2}\left(\frac{r_y}{N_y}-1\right)-\frac{1}{3N_y}\right)\rho_2^{N_x\times N_y}(r_x,r_y+1;t)\\ &+P_{g_x}\left(-\frac{1}{2}+\frac{N_x}{6}-\frac{r_x}{2}\left(\frac{r_x}{N_x}-1\right)-\frac{1}{3N_x}\right)\rho_2^{N_x\times N_y}(r_x-1,r_y;t)\\ &+P_{g_x}\left(-\frac{1}{2}+\frac{N_x}{6}-\frac{r_x}{2}\left(\frac{r_x}{N_x}-1\right)-\frac{1}{3N_x}\right)\rho_2^{N_x\times N_y}(r_x+1,r_y;t). \qquad (22)\end{aligned}$$

If we compare Eqs. (17) and (20)-(22) it is apparent that the length of the domain influences the evolution of the pairwise density functions in the case of GM2, but not in GM1. Therefore we expect the evolution of the pairwise density functions to be affected by the initial domain size in the case of GM2, but not GM1.

3 Results

We initially present results for immotile, non-proliferative agents on a growing domain, in which domain growth is exponential. We simulate the scenario in which all lattice sites are occupied by an agent in the IBM on a lattice of size 100 by 100 sites. This means the initial conditions for Eqs. (17) and (20)-(22) are

$$c(0) = 1, \qquad (23)$$

and

$$\rho_2^{N_x\times N_y}(r_x,r_y;0) = 1, \quad \forall\, r_x < N_x, r_y < N_y. \qquad (24)$$

As previously stated, N_x and N_y describe the number of lattice sites in the horizontal and vertical directions, respectively. However, as results from the IBM are ensemble averages we substitute N_x and N_y for their continuum analogues $L_x(t)$ and $L_y(t)$, respectively. For exponential domain

bioRxiv preprint doi: https://doi.org/10.1101/041509; this version posted February 26, 2016. The copyright holder for this preprint (which was not certified by peer review) is the author/funder. All rights reserved. No reuse allowed without permission.

growth $L_x(t)$ evolves according to

$$\frac{\mathrm{d}L_x(t)}{\mathrm{d}t} = P_{g_x} L_x(t). \tag{25}$$

The evolution of $L_y(t)$ is equivalent. This substitution of $N_x(t)$ and $N_y(t)$ with $L_x(t)$ and $L_y(t)$ avoids jump discontinuities in the numerical solutions of Eqs. (17) and (20)-(22), which are not present in the averaged IBM results. To solve our equations numerically we use MATLAB's `ode15s`.

3.1 Agents on a growing domain

In Fig. 3 the numerical solutions of Eqs. (17) and (20)-(22) are shown for the evolution of the pairwise density functions on a growing domain. In Fig. 3 (a) we see the evolution of the pairwise density functions for GM1, and the difference in the evolution of the colinear and diagonal components, as we would expect. In the absence of agent motility and proliferation the evolution of the pairwise density functions for all colinear distances (i.e. Δ, 2Δ, 3Δ, ...) is the same for GM1, this is also the case for the diagonal component. Conversely, In Fig. 3 (b) we see the evolution of the pairwise density functions for GM2, and in this case in the evolution of all the colinear and diagonal components is the same.

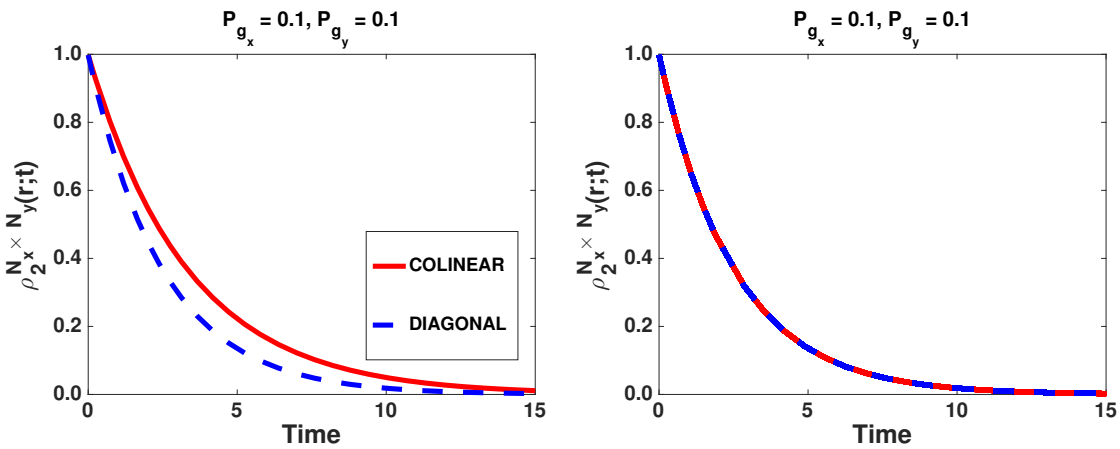

(a) (b)

Figure 3: (Colour online): The evolution of the colinear and diagonal components of the pairwise density functions for (a) GM1 and (b) GM2.

bioRxiv preprint doi: https://doi.org/10.1101/041509; this version posted February 26, 2016. The copyright holder for this preprint (which was not certified by peer review) is the author/funder. All rights reserved. No reuse allowed without permission.

3.2 Agent motility, proliferation and death

It has previously been shown how to include the effect of agent motility and proliferation in Eqs. (9), (17), and (20)-(22) and so we refer the reader to Appendix B for the derivation and simply state the result for the individual density function here [25, 38, 39]. The evolution of the individual density function for motile and proliferating agents on a growing domain is

$$\frac{\mathrm{d}c(t)}{\mathrm{d}t} = P_p(c(t) - \rho_2^{N_x \times N_y}(1, 0; t)) - (P_{g_x} + P_{g_y})c(t). \tag{26}$$

Correlation functions

To make our results comparable with the large amount of research already completed in this area we display the results in terms of the correlation function [25, 31–39]. The correlation function [34, 35] is simply defined as

$$F(r_x, r_y; t) := \frac{\rho_2^{N_x \times N_y}(r_x, r_y; t)}{c(t)^2}. \tag{27}$$

The correlation function is a useful variable to work with as $F \equiv 1$ means that the occupancy of two lattice sites a given distance apart is independent. If we substitute Eq. (27) into Eq. (26) we obtain

$$\frac{\mathrm{d}c(t)}{\mathrm{d}t} = P_p c(t)(1 - F(1, 0; t)c(t)) - (P_{g_x} + P_{g_y})c(t). \tag{28}$$

The standard MFA assumes $F(1, 0; t) = 1$, and so is

$$\frac{\mathrm{d}c(t)}{\mathrm{d}t} = P_p c(t)(1 - c(t)) - (P_{g_x} + P_{g_y})c(t). \tag{29}$$

For the IBM in all simulations we have an initial uniform random seeding of density 0.05. The lattice state of site i of the two-dimensional IBM is described by variable σ_i (i.e. occupied by an agent or unoccupied). This means the normalised average agent density for the two-dimensional domain is

$$c(t) = \frac{1}{N_x(t)N_y(t)} \sum_{i}^{N_x(t)N_y(t)} \mathbb{1}_A\{\sigma_i\}. \tag{30}$$

bioRxiv preprint doi: https://doi.org/10.1101/041509; this version posted February 26, 2016. The copyright holder for this preprint (which was not certified by peer review) is the author/funder. All rights reserved. No reuse allowed without permission.

Here $\mathbb{1}_A$ is the indicator function for species A (i.e. 1 if species A occupies site i, and 0 if it does not). As previously discussed, the initial condition in the IBM is achieved by populating a certain number of sites uniformly at random until the initial density is achieved, the initial condition for the correlation function is therefore

$$F(r_x, r_y; 0) = 1, \quad \forall\ r_x < N_x, r_y < N_y. \tag{31}$$

that is, at all distances there are initially no spatial correlations between agents. We also rescale time to allow for ease of comparison between simulations with different parameters:

$$\bar{t} = (P_p - P_d - (P_{g_x} + P_{g_y}))t. \tag{32}$$

The rescaling of time is necessary to allow the easy comparison of simulations with different parameters. As before we solve our equations numerically with MATLAB's `ode15s`.

3.3 Agent motility and proliferation

In Fig. 4 the effects of domain growth via GM1 on the evolution of the macroscopic agent density can be seen. We see that the inclusion of GM1 causes the steady-state density predicted by the standard MFA, Eq. (29), to be incorrect. The steady-state density calculated from an ensemble average from the IBM is lower than the MFA predicts, which the correlation ODE model (Eq. (28)) is able to capture. The rate at which the agent density increases is also reduced in the IBM due to spatial correlations, and the correlations ODE model better approximates this than the MFA. One may expect domain growth to decrease spatial correlations by 'breaking-up' existing agent clusters which, in turn, would allow greater agent movement and cause the MFA to be more accurate. However, the nature of GM1 means that it does not break up agents effectively, only potentially 'freeing-up' one lattice site for two agents in each row/column every growth event (see Fig. 1). GM1 also does not cause agents to make new neighbouring agents, with agents and their neighbours moving synchronously in a growth event (except at the position of growth where two columns/rows will be separated). Therefore, the spatial correlations associated with agent proliferation (in conjunction with the dilution of agent density due to domain growth) lower the steady-state density of the agents more than

bioRxiv preprint doi: https://doi.org/10.1101/041509; this version posted February 26, 2016. The copyright holder for this preprint (which was not certified by peer review) is the author/funder. All rights reserved. No reuse allowed without permission.

the displacement of agents by domain growth counteracts the spatial correlations established by agent proliferation.

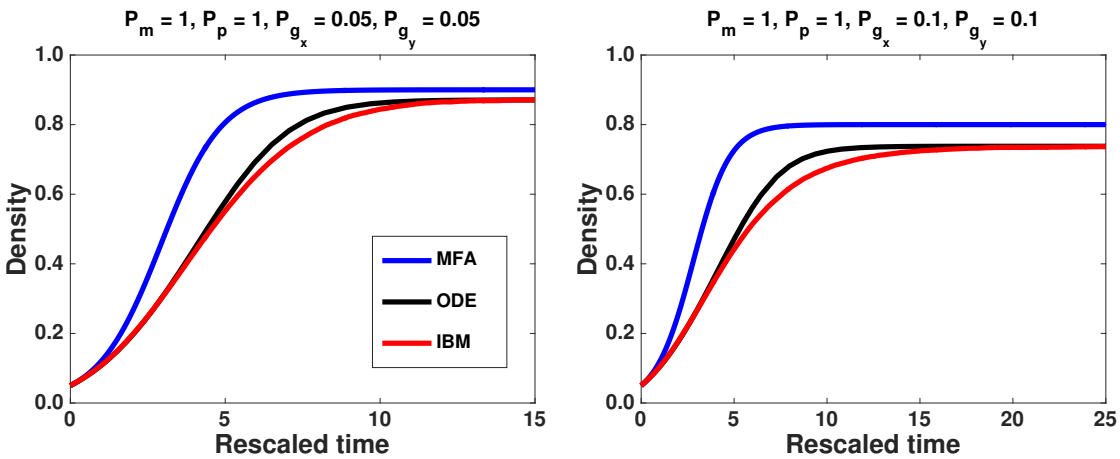

(a) (b)

Figure 4: (Colour online): For GM1 including pairwise correlations in a correlation ODE model provides a more accurate approximation of the evolution of the macroscopic density in the IBM than the MFA.

In Figs. 5 and 6 the effect of GM1 on spatial correlations in both the correlation ODE model and the IBM can be seen. Importantly, we see that as the growth rate is increased the spatial correlations augment. From Fig. 4 this result is to be expected, as domain growth lowers the agent steady-state density but is not effective at reducing spatial correlations. A similar result has previously been observed in the case of agent death [25]. In addition, at the agent steady-state density the spatial correlations do not return to $F = 1$. This explains why the MFA incorrectly predicts the agent steady-state density, and shows why the correlation ODE model is able to correctly approximate the steady-state density of the IBM. This is because the MFA is only correct when $F = 1$, which is not the case in the IBM in this scenario with GM1.

bioRxiv preprint doi: https://doi.org/10.1101/041509; this version posted February 26, 2016. The copyright holder for this preprint (which was not certified by peer review) is the author/funder. All rights reserved. No reuse allowed without permission.

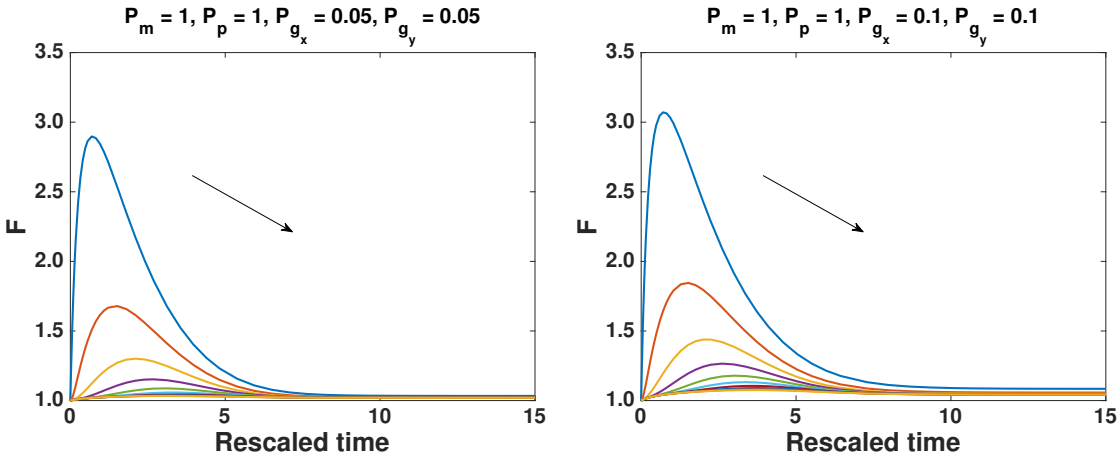

(a) (b)

Figure 5: (Colour online): Increasing the growth rates, P_{g_x} and P_{g_y}, causes the pairwise correlations to augment for GM1 in the correlation ODE model (compare (a) with (b)). In the case of GM1, the pairwise correlations do not return to $F = 1$. The distance increases from Δ to 10Δ in steps of Δ. Increasing distance is from top to bottom as indicated by the arrows.

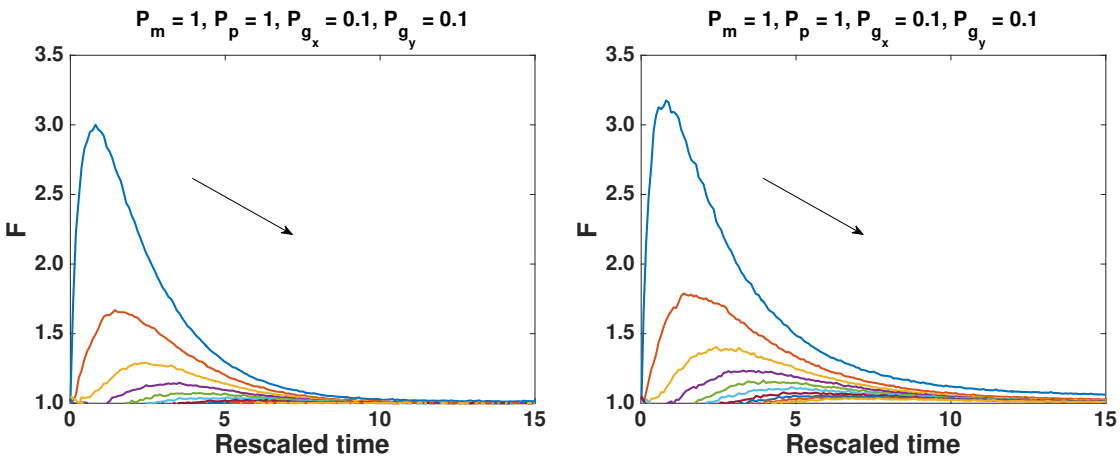

(a) (b)

Figure 6: (Colour online): Increasing the growth rate, P_{g_x} and P_{g_y}, causes the pairwise correlations to augment for GM1 in the IBM. In the case of GM1, the pairwise correlations do not return to $F = 1$. The distance increases from Δ to 10Δ in steps of Δ. Increasing distance is from top to bottom as indicated by the arrows.

bioRxiv preprint doi: https://doi.org/10.1101/041509; this version posted February 26, 2016. The copyright holder for this preprint (which was not certified by peer review) is the author/funder. All rights reserved. No reuse allowed without permission.

In Fig. 7 the effect of domain growth via GM2 on agent density can be seen. In this case we see that GM2 causes the steady-state density predicted by the MFA to be correct. This is because GM2 is more effective at breaking up agent clusters than GM1, potentially 'freeing-up' one lattice site for four agents in each row/column every growth event. This counteracts the effect of the spatial correlations created by agent proliferation. GM2 also causes agents to change neighbouring agents in the IBM, and so further reduces the spatial correlations associated with agent proliferation. Despite this we see that the correlations ODE model still more accurately predicts the rate at which the agent density evolves, while also accurately approximating the steady-state density in the IBM.

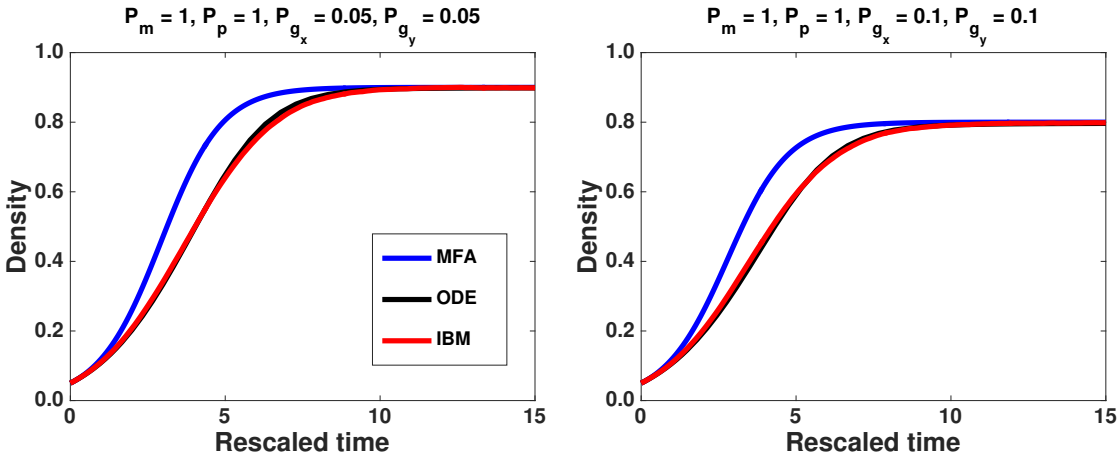

(a) (b)

Figure 7: (Colour online): For GM2 including pairwise correlations in a correlation ODE model provides a more accurate approximation of the results of the evolution of the macroscopic density in the IBM.

In Figs. 8 and 9 the effect of GM2 on spatial correlations can be seen in both the correlations ODE model and calculated directly from the IBM. In contrast to GM1 we see that as the growth rate is increased the spatial correlations decrease. We also see that at the steady-state density $F = 1$, this provides the reason as to why the agent steady-state predicted by the MFA is correct.

bioRxiv preprint doi: https://doi.org/10.1101/041509; this version posted February 26, 2016. The copyright holder for this preprint (which was not certified by peer review) is the author/funder. All rights reserved. No reuse allowed without permission.

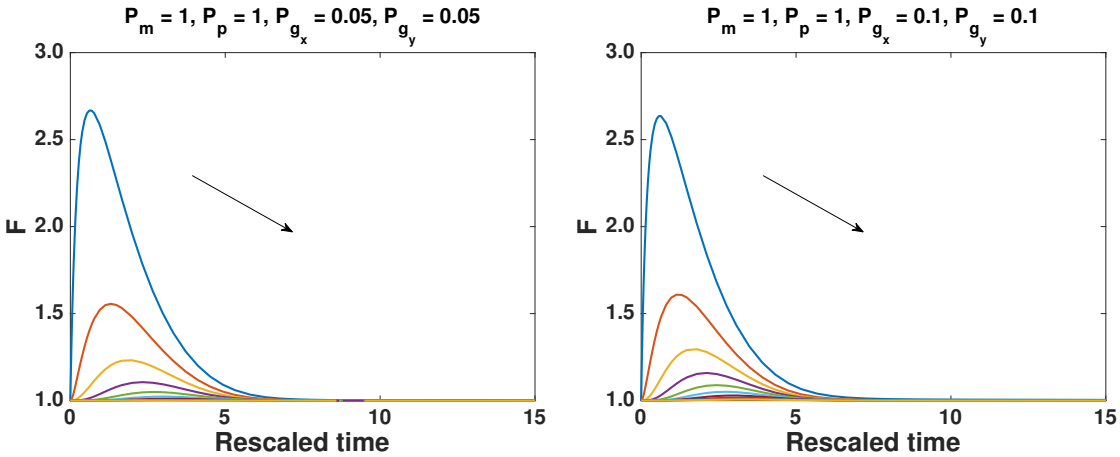

(a) (b)

Figure 8: (Colour online): For GM2 increasing the growth rate, P_{g_x} and P_{g_y}, causes the pairwise correlations to shrink. In the case of GM2, the pairwise correlations return to $F = 1$. The distance increases from Δ to 10Δ in steps of Δ. Increasing distance is from top to bottom as indicated by the arrows.

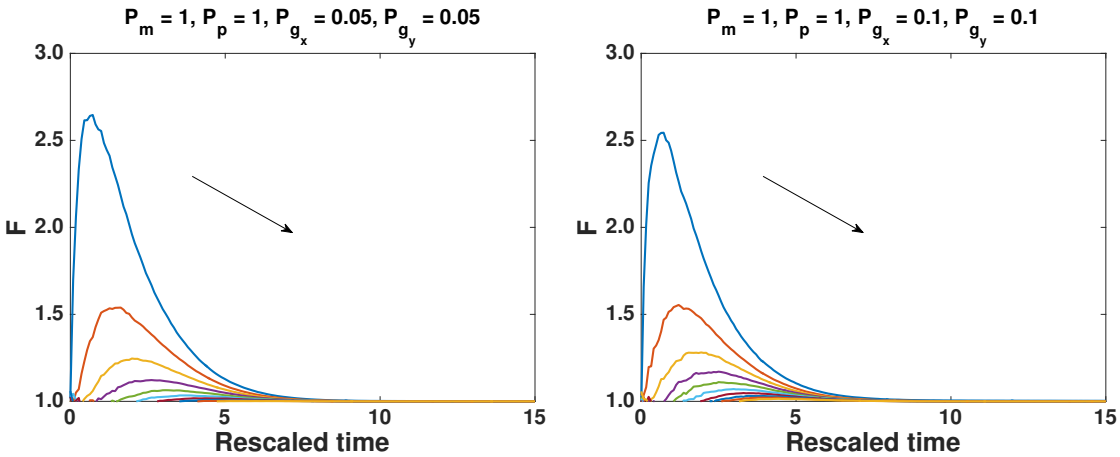

(a) (b)

Figure 9: (Colour online): Increasing the growth rate, P_{g_x} and P_{g_y}, causes the pairwise correlations to shrink for GM2 in the IBM. The distance increases from Δ to 10Δ in steps of Δ. Increasing distance is from top to bottom as indicated by the arrows.

bioRxiv preprint doi: https://doi.org/10.1101/041509; this version posted February 26, 2016. The copyright holder for this preprint (which was not certified by peer review) is the author/funder. All rights reserved. No reuse allowed without permission.

In Figs. 10 and 11 we can see that the size of the domain influences the evolution of the agent density in the case of GM2, but not in the case of GM1. In the case of GM2, as the initial domain size is increased the evolution of the macroscopic agent density is accelerated. This is because colinear spatial correlations, established by agent proliferation, are broken down proportional to the domain size in GM2. This can be seen most easily by converting Eq. (21) from discrete to continuous variables, that is $r_x = x/\Delta$, $r_y = y/\Delta$, $N_x = L_x/\Delta$ and $N_y = L_y/\Delta$:

$$\begin{aligned}\frac{\mathrm{d}\rho_2^{N_x\times N_y}(x,0;t)}{\mathrm{d}t} &= -P_{g_x}\left(\frac{x}{\Delta}+1\right)\rho_2^{N_x\times N_y}(x,0;t)\\ &+ P_{g_x}\left(\frac{x}{\Delta}-1\right)\rho_2^{N_x\times N_y}(x-\Delta,0;t)\\ &+ P_{g_y}\left(-1-\frac{L_y}{3\Delta}+\frac{\Delta}{3L_y}\right)\rho_2^{N_x\times N_y}(x,0;t)\\ &+ P_{g_y}\left(-1+\frac{L_y}{3\Delta}+\frac{2\Delta}{3L_y}\right)\rho_2^{N_x\times N_y}(x,\Delta;t). \end{aligned} \tag{33}$$

If we Taylor series expand around x and y in Eq. (33) we obtain

$$\begin{aligned}\frac{\partial\rho_2^{N_x\times N_y}(x,0;t)}{\partial t} &= -P_{g_x}\left(\frac{x}{\Delta}+1\right)\rho_2^{N_x\times N_y}(x,0;t)\\ &+ P_{g_x}\left(\frac{x}{\Delta}-1\right)\left[\rho_2^{N_x\times N_y}(x,0;t)-\Delta\frac{\partial\rho_2^{N_x\times N_y}(x,0;t)}{\partial x}+\mathcal{O}(\Delta^2)\right]\\ &+ P_{g_y}\left(-1-\frac{L_y}{3\Delta}+\frac{\Delta}{3L_y}\right)\rho_2^{N_x\times N_y}(x,0;t)\\ &+ P_{g_y}\left(-1+\frac{L_y}{3\Delta}+\frac{2\Delta}{3L_y}\right)\left[\rho_2^{N_x\times N_y}(x;t)+\Delta\frac{\partial\rho_2^{N_x\times N_y}(x;t)}{\partial y}+\mathcal{O}(\Delta^2)\right]. \end{aligned} \tag{34}$$

If we then simplify Eq. (34) and take the limit as $\Delta \to 0$ we arrive at

$$\begin{aligned}\frac{\partial\rho_2^{N_x\times N_y}(x,0;t)}{\partial t} &= -2P_{g_x}\rho_2^{N_x\times N_y}(x,0;t)-2P_{g_y}\rho_2^{N_x\times N_y}(x,0;t)-P_{g_x x}\frac{\partial\rho_2^{N_x\times N_y}(x,0;t)}{\partial x}\\ &+\frac{P_{g_y}L_y}{3}\frac{\partial\rho_2^{N_x\times N_y}(x,0;t)}{\partial y}. \end{aligned} \tag{35}$$

The final term on the RHS of Eq. (35) shows that horizontally colinear lattice sites are separated at a rate dependent on the length of the domain perpendicular to the row/column of the lattice sites in GM2. This is what causes the initial size of the domain to influence the evolution of the agent density in GM2.

bioRxiv preprint doi: https://doi.org/10.1101/041509; this version posted February 26, 2016. The copyright holder for this preprint (which was not certified by peer review) is the author/funder. All rights reserved. No reuse allowed without permission.

Finally, in Figs. 12 and 13 we see the initial domain size also impacts the evolution of the spatial correlations for GM2, but not for GM1. In the case of GM2 as the initial domain size is increased the spatial correlations between agents are reduced.

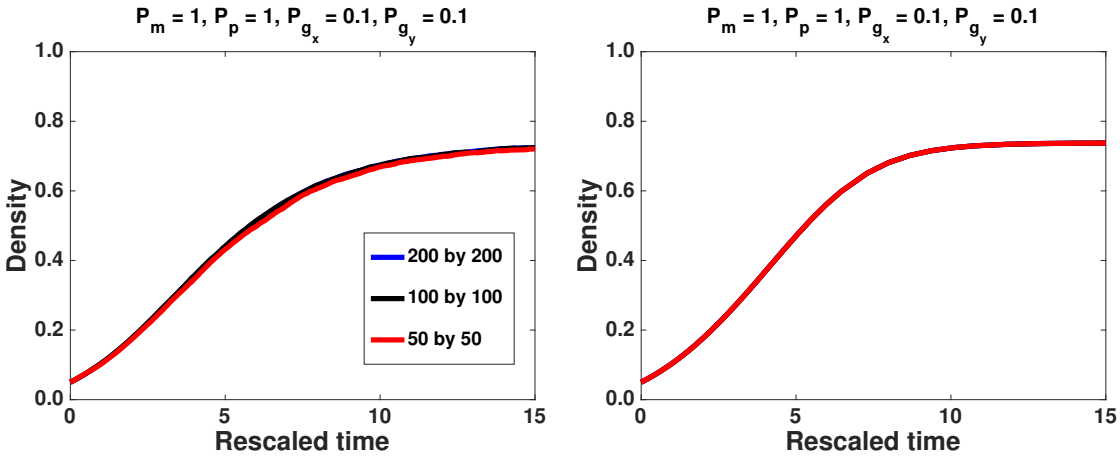

(a) (b)

Figure 10: (Colour online): Altering the initial domain size does not cause the evolution of the agent density to change in GM1. As the initial size of the domain is increased, from 50 by 50 to 200 by 200 lattice sites, the evolution of the agent density to steady-state remains the same in GM1. (a) IBM and (b) correlation ODE model.

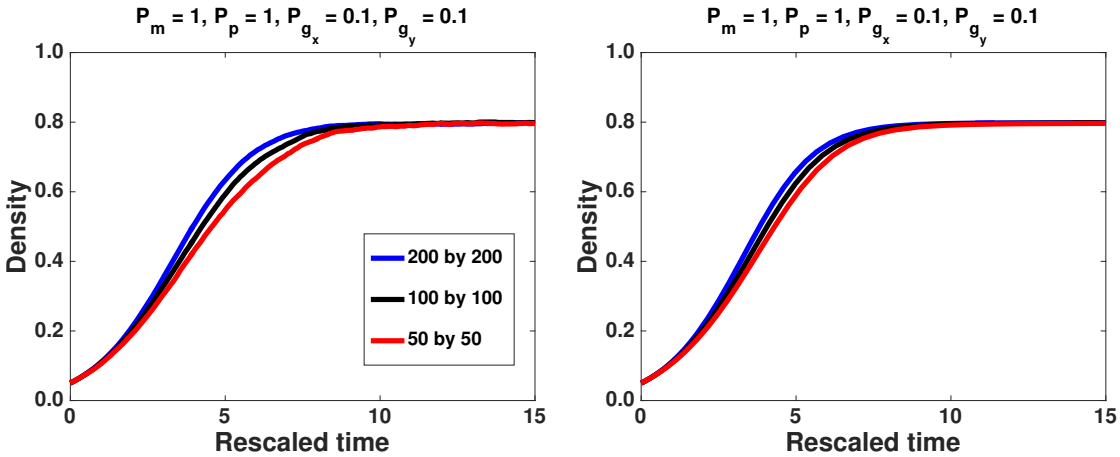

(a) (b)

Figure 11: (Colour online): Altering the initial domain size causes the evolution of the agent density to change in GM2. As the initial size of the domain is increased, from 50 by 50 to 200 by 200 lattice sites, the evolution of the agent density accelerates in GM2. (a) IBM and (b) correlation ODE model.

bioRxiv preprint doi: https://doi.org/10.1101/041509; this version posted February 26, 2016. The copyright holder for this preprint (which was not certified by peer review) is the author/funder. All rights reserved. No reuse allowed without permission.

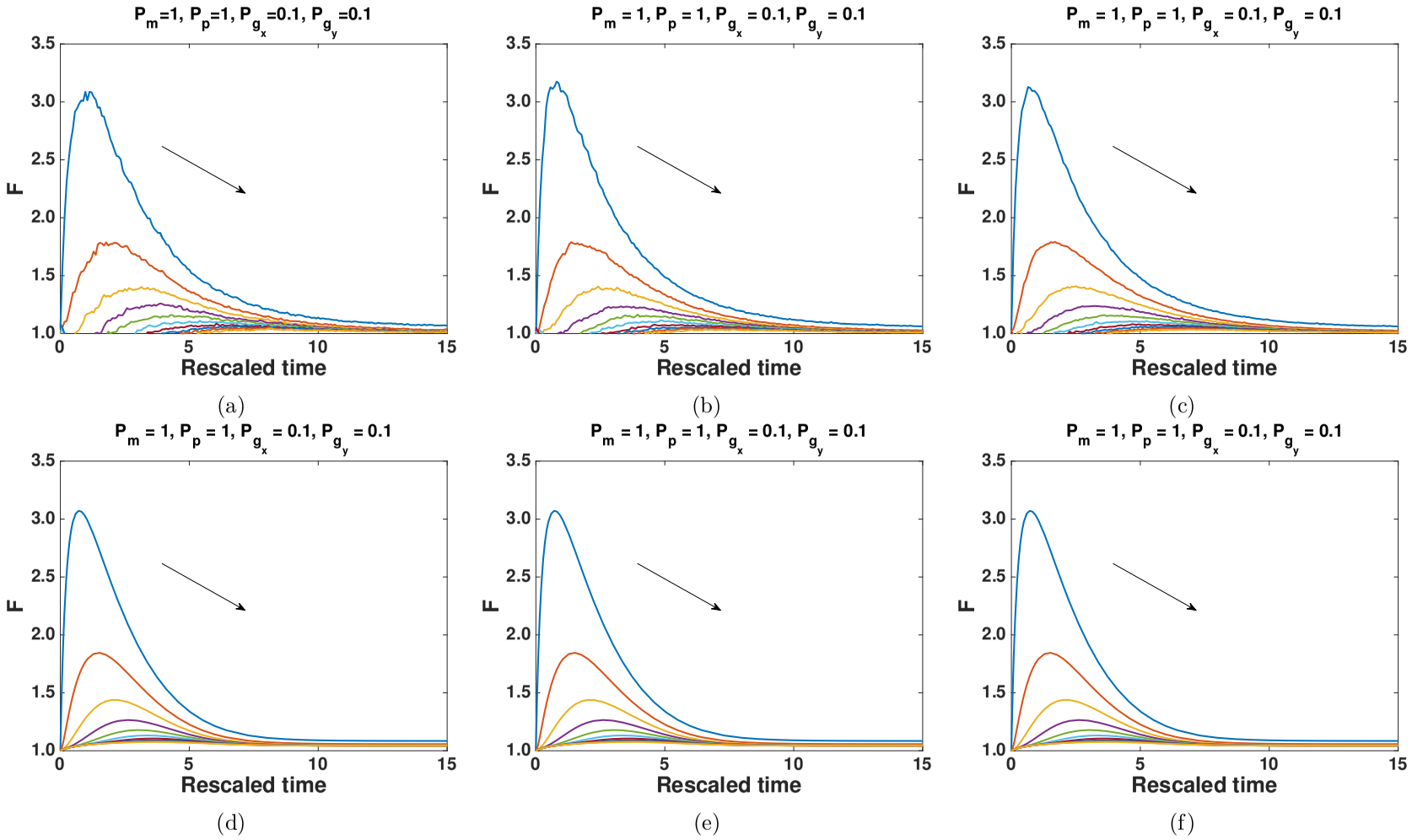

Figure 12: (Colour online): Altering the initial size of the domain does not change the evolution of the pairwise correlations in the case of GM1. (a-c) IBM, 50 by 50, 100 by 100, 200 by 200. (d-f) correlation ODE model 50 by 50, 100 by 100, 200 by 200. Increasing distance is from top to bottom as indicated by the arrows.

bioRxiv preprint doi: https://doi.org/10.1101/041509; this version posted February 26, 2016. The copyright holder for this preprint (which was not certified by peer review) is the author/funder. All rights reserved. No reuse allowed without permission.

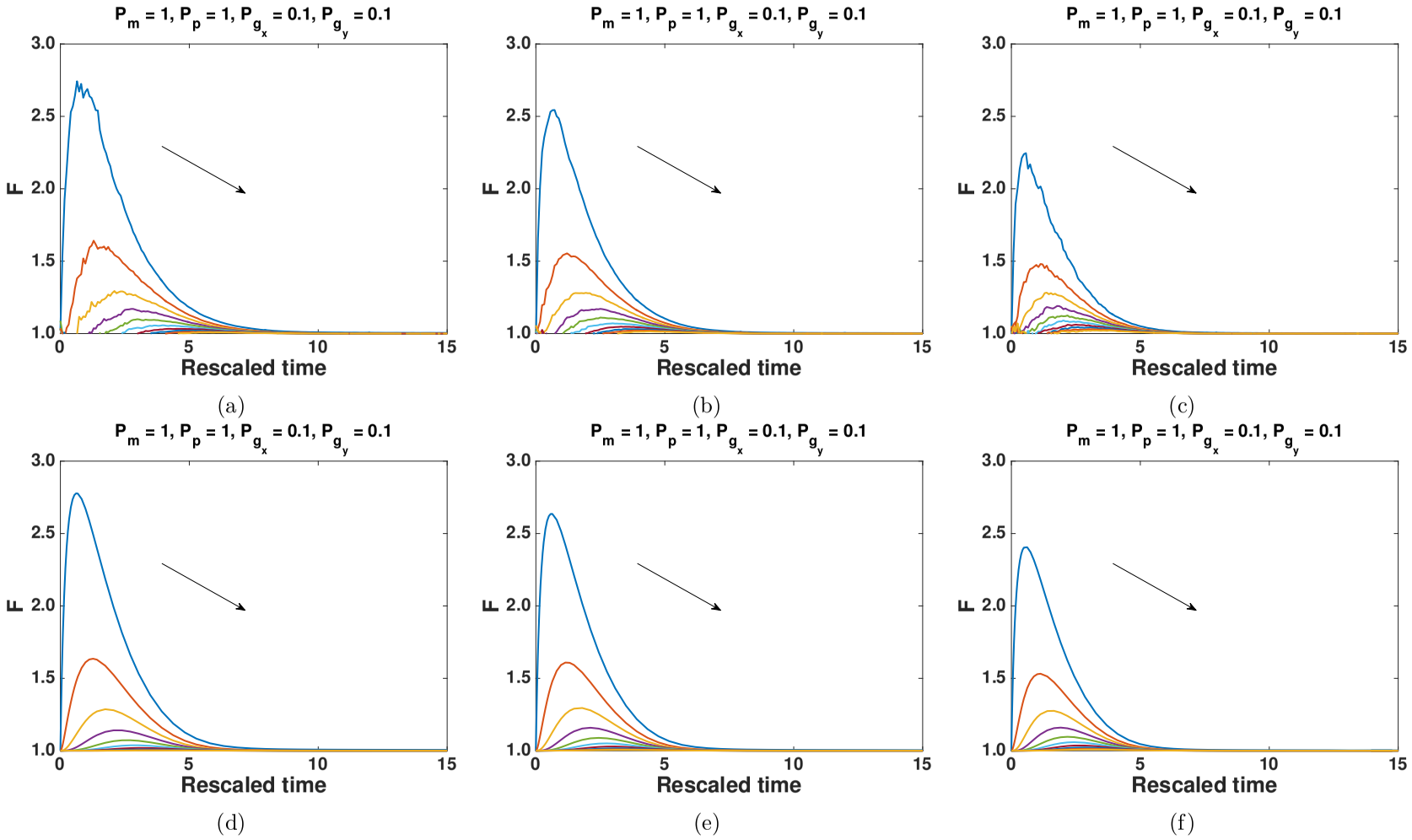

Figure 13: (Colour online): Altering the initial size of the domain changes the evolution of the pairwise correlations in the case of GM2. In the case of GM2 the correlations are reduced as the initial domain size becomes larger. (a-c) IBM, 50 by 50, 100 by 100, 200 by 200. (d-f) correlation ODE model 50 by 50, 100 by 100, 200 by 200. Increasing distance is from top to bottom as indicated by the arrows.

bioRxiv preprint doi: https://doi.org/10.1101/041509; this version posted February 26, 2016. The copyright holder for this preprint (which was not certified by peer review) is the author/funder. All rights reserved. No reuse allowed without permission.

4 Discussion and conclusion

The importance of accurately including the effect of domain growth in models of biological phenomena is becoming increasingly apparent [1, 2, 6, 14–17]. Many of the fundamental developmental processes that determine mammalian morphology are either characterised by growth, or occur during it, and so it is possible that growth may play an important role in determining and coordinating cell population behaviour [3, 9].

In this work we have studied two different implementations of domain growth. We chose two different, yet potentially biologically relevant growth mechanisms [44–46], to highlight how understanding the form of domain growth is crucial. These growth mechanisms originated from thinking about the different ways in which new sites could be added to the IBM domain, and the consequences this may have on agent density. As has been shown in this work, GM1 is an implementation of domain growth that conserves colinear correlations in comparison to diagonal correlations, and GM2 is one that reduces colinear correlations as a rate proportional to the size of the domain. This difference between GM1 and GM2 is why GM2 exhibits a length dependency and GM1 does not.

It is important to acknowledge that we have only looked at scenarios where $P_p = P_m$. This is a very high rate of proliferation with respect to motility. However, we chose these parameters to effectively test the accuracy of our correlation ODE model. In situations where $P_p < P_m$, the correlation ODE model increases in accuracy in terms of approximating the IBM results, as has been shown previously [25, 39]. It is also important to recognise that all domain growth has been two-dimensional and, as would be expected, different IBM behaviour is observed with one-dimensional growth of a two-dimensional domain with equivalent parameter values to those used here. This does pose the question as to whether two-dimensional growth via GM1 is realistic. In this work we have used GM1 as an extreme example of growth in which the cell cycles of adjacent cells that are causing the domain to grow are synchronous [46]. In reality, it is unlikely that domain growth in biological systems is captured by algorithms as simple as GM1 and GM2. However, it stands to reason that more realistic growth mechanisms may exist that exhibit similar effects on spatial correlations as GM1 and GM2. We have also only looked

bioRxiv preprint doi: https://doi.org/10.1101/041509; this version posted February 26, 2016. The copyright holder for this preprint (which was not certified by peer review) is the author/funder. All rights reserved. No reuse allowed without permission.

at the case when $P_{g_x} = P_{g_y}$. We did this to reduce the complexity of solving the equations, however, the results presented here could be extended to cases where $P_{g_x} \neq P_{g_y}$.

Acknowledgements

RJHR would like to thank the UK's Engineering and Physical Sciences Research Council (EPSRC) for funding through a studentship at the Systems Biology programme of the University of Oxford's Doctoral Training Centre. The authors would also like to thank Matthew Simpson and Deborah Markham for useful discussions.

bioRxiv preprint doi: https://doi.org/10.1101/041509; this version posted February 26, 2016. The copyright holder for this preprint (which was not certified by peer review) is the author/funder. All rights reserved. No reuse allowed without permission.

References

[1] P. J. Keller. Imaging morphogenesis: Technological advances and biological insights. *Science*, 340(6137), 2013.

[2] A. Aman and T. Piotrowski. Cell migration during morphogenesis. *Developmental Biology*, 341(1):20–33, 2010.

[3] L. Wolpert. *Principles of Development*. Oxford University Press, Oxford, 4th edition, 2011.

[4] J. S. Kim, J. Min, A. K. Recknagel, M. Riccio, and J. T. Butcher. Quantitative three-dimensional analysis of embryonic chick morphogenesis via microcomputed tomography. *The Anatomical Record: Advances in Integrative Anatomy and Evolutionary Biology*, 294 (1):1–10, 2011.

[5] T. E. Woolley, R. E. Baker, C. Tickle, P. K. Maini, and M. Towers. Mathematical modelling of digit specification by a sonic hedgehog gradient. *Developmental Dynamics*, 243(2):290–298, 2014.

[6] R. McLennan, L. Dyson, K. W. Prather, J. A. Morrison, R. E. Baker, P. K. Maini, and P. M. Kulesa. Multiscale mechanisms of cell migration during development: theory and experiment. *Development*, 139(16):2935–2944, 2012.

[7] R. McLennan, L. J. Schumacher, J. A. Morrison, J. M. Teddy, D. A. Ridenour, A. C. Box, C. L. Semerad, H. Li, W. McDowell, D. Kay, P. K. Maini, R. E. Baker, and P. M. Kulesa. Neural crest migration is driven by a few trailblazer cells with a unique molecular signature narrowly confined to the invasive front. *Development*, 142(11):2014–2025, 2015.

[8] R. McLennan, L. J. Schumacher, J. A. Morrison, J. M. Teddy, D. A. Ridenour, A. C. Box, C. L. Semerad, H. Li, W. McDowell, D. Kay, P. K. Maini, R. E. Baker, and P. M. Kulesa. VEGF signals induce trailblazer cell identity that drives neural crest migration. *Developmental Biology*, 407(1):12–25, 2015.

[9] R. L. Mort, R. J. H. Ross, K. J. Hainey, O. Harrison, M. A. Keighren, G. Landini, R. E. Baker, K. J. Painter, I. J. Jackson, and C. A. Yates. Reconciling diverse mammalian

bioRxiv preprint doi: https://doi.org/10.1101/041509; this version posted February 26, 2016. The copyright holder for this preprint (which was not certified by peer review) is the author/funder. All rights reserved. No reuse allowed without permission.

pigmentation patterns with a fundamental mathematical model. *Nature Communications*, 7(10288), 2016.

[10] B. J. Binder, K. A. Landman, M. J. Simpson, M. Mariani, and D. F. Newgreen. Modeling proliferative tissue growth: A general approach and an avian case study. *Physical Review E*, 78(3):031912, 2008.

[11] M. Lampl. Perspectives on modelling human growth: Mathematical models and growth biology. *Annals of Human Biology*, 39(5):342–351, 2012.

[12] S. Perilli, R. Di Mambro, and S. Sabatini. Growth and development of the root apical meristem. *Current Opinion in Plant Biology*, 15(1):17–23, 2012.

[13] J. F. Fallon, A. Lopez, M. A. Ros, M. P. Savage, B. B. Olwin, and B. K. Simandl. FGF-2: apical ectodermal ridge growth signal for chick limb development. *Science*, 264(5155): 104–107, 1994.

[14] R. Kennaway, E. Coen, A. Green, and A. Bangham. Generation of diverse biological forms through combinatorial interactions between tissue polarity and growth. *PLoS Computational Biology*, 7(6):e1002071, 2011.

[15] P. Fried and D. Iber. Dynamic scaling of morphogen gradients on growing domains. *Nature Communications*, 5(5077), 2014.

[16] E. J. Crampin, E. A. Gaffney, and P. K. Maini. Reaction and diffusion on growing domains: Scenarios for robust pattern formation. *Bulletin of Mathematical Biology*, 61(6):1093–1120, 1999.

[17] R. E. Baker, C. A. Yates, and R. Erban. From microscopic to macroscopic descriptions of cell migration on growing domains. *Bulletin of Mathematical Biology*, 72(3):719–762, 2010.

[18] C. A. Yates. Discrete and continuous models for tissue growth and shrinkage. *Journal of Theoretical Biology*, 350:37–48, 2014.

[19] S. Azaele, A. Maritan, S. J. Cornell, S. Suweis, J. R. Banavar, D. Gabriel, and W. E. Kunin. Towards a unified descriptive theory for spatial ecology: predicting biodiversity patterns across spatial scales. *Methods in Ecology and Evolution*, 6(3):324–332, 2015.

bioRxiv preprint doi: https://doi.org/10.1101/041509; this version posted February 26, 2016. The copyright holder for this preprint (which was not certified by peer review) is the author/funder. All rights reserved. No reuse allowed without permission.

[20] P. C. Lai, C. M. Wong, A. J. Hedley, S. V. Lo, P. Y. Leung, J. Kong, and G. M. Leung. Understanding the spatial clustering of severe acute respiratory syndrome (SARS) in Hong Kong. *Environmental Health Perspectives*, 112(15):1550—1556, 2004.

[21] B. J. Binder, K. A. Landman, D. F. Newgreen, J. E. Simkin, Y. Takahashi, and D. Zhang. Spatial analysis of multi-species exclusion processes: application to neural crest cell migration in the embryonic gut. *Bulletin of Mathematical Biology*, 74(2):474–90, 2012.

[22] B. J. Binder and M. J. Simpson. Quantifying spatial structure in experimental observations and agent-based simulations using pair-correlation functions. *Physical Review E*, 88(2): 022705, 2013.

[23] D. J. G. Agnew, J. E. F. Green, T. M. Brown, M. J. Simpson, and B. J. Binder. Distinguishing between mechanisms of cell aggregation using pair-correlation functions. *Journal of Theoretical Biology*, 352:16–23, 2014.

[24] B. Waclaw, I. Bozic, M. E. Pittman, R. H. Hruban, B. Vogelstein, and M. A. Nowak. A spatial model predicts that dispersal and cell turnover limit intratumour heterogeneity. *Nature*, 525(7568):261–264, 2015.

[25] R. E. Baker and M. J. Simpson. Correcting mean-field approximations for birth-death-movement processes. *Physical Review E*, 82(4):041905, 2010.

[26] B. J. Binder and K. A. Landman. Exclusion processes on a growing domain. *Journal of Theoretical Biology*, 259(3):541–551, 2009.

[27] A. E. Fernando, K. A. Landman, and M. J. Simpson. Nonlinear diffusion and exclusion processes with contact interactions. *Physical Review E*, 81(1):011903, 2010.

[28] E. Khain, L. M. Sander, and C. M. Schneider-Mizell. The role of cell-cell adhesion in wound healing. *Journal of Statistical Physics*, 128(1-2):209–218, 2007.

[29] K. A. Landman and A. E. Fernando. Myopic random walkers and exclusion processes: Single and multispecies. *Physica A*, 390(21-22):3742–3753, 2011.

[30] M. J. Simpson, K. A. Landman, and B. D. Hughes. Pathlines in exclusion processes. *Physical Review E*, 79(3):031920, 2009.

bioRxiv preprint doi: https://doi.org/10.1101/041509; this version posted February 26, 2016. The copyright holder for this preprint (which was not certified by peer review) is the author/funder. All rights reserved. No reuse allowed without permission.

[31] M. A. M. de Aguiar, E. M. Rauch, and Y. Bar-Yam. Invasion and extinction in the mean-field approximation for a spatial host-pathogen model. *Journal of Statistical Physics*, 114 (5–6):1417–1451, 2004.

[32] D. Hiebeler. Stochastic spatial models: From simulations to mean-field and local structure approximations. *Journal of Theoretical Biology*, 187(3):307–319, 1997.

[33] H. Fukś and A. T. Lawniczak. Individual-based lattice model for spatial spread of epidemics. *Discrete Dynamics in Nature and Society*, 6(3):191–200, 2001.

[34] J. Mai, V. N. Kuzovkov, and W. von. Niessen. A theoretical stochastic model for the $A+\frac{1}{2}B \rightarrow 0$ reaction. *Journal of Chemical Physics*, 98(12):10017, 1993.

[35] J. Mai, V. N. Kuzovkov, and W. von. Niessen. A general stochastic model for the description of surface reaction systems. *Physica A*, 203:298–315, 1994.

[36] M. J. Simpson and R. E. Baker. Corrected mean-field models for spatially dependent advection-diffusion-reaction phenomena. *Physical Review E*, 83(5):051922, 2011.

[37] S. T. Johnston, M. J. Simpson, and R. E. Baker. Mean-field descriptions of collective migration with strong adhesion. *Physical Review E*, 85(5):051922, 2012.

[38] D. C. Markham, M. J. Simpson, P. K. Maini, E. A. Gaffney, and R. E. Baker. Incorporating spatial correlations into multispecies mean-field models. *Physical Review E*, 88(5):052713, 2013.

[39] D. C. Markham, M. J. Simpson, and R. E. Baker. Simplified method for including spatial correlations in mean-field approximations. *Physical Review E*, 87(6):062702, 2013.

[40] T. M. Liggett. *Stochastic Interacting Systems: Contact, Voter, and Exclusion Processes.* Springer-Verlag, Berlin, 1999.

[41] M. J. Simpson, K. A. Landman, and B. D. Hughes. Cell invasion with proliferation mechanisms motivated by time-lapse data. *Physica A*, 389(18):3779 – 3790, 2010.

[42] M. J. Simpson, A. Merrifield, K. A. Landman, and B. D. Hughes. Simulating invasion with cellular automata: Connecting cell-scale and population-scale properties. *Physical Review E*, 76:021918, Aug 2007.

bioRxiv preprint doi: https://doi.org/10.1101/041509; this version posted February 26, 2016. The copyright holder for this preprint (which was not certified by peer review) is the author/funder. All rights reserved. No reuse allowed without permission.

[43] D. T. Gillespie. Exact stochastic simulaton of coupled chemical reactions. *Journal of Physical Chemistry*, 81(25):2340–2361, 1977.

[44] B. J. Thomas, D. A. Gunning, J. Cho, and S. L. Zipursky. Cell cycle progression in the developing Drosophila eye: *roughex* encodes a novel protein required for the establishment of G1. *Cell*, 77(7):1003–1014, 1994.

[45] J. P. Kumar. My what big eyes you have: How the Drosophila retina grows. *Developmental Neurobiology*, 71(12):1133–1152, 2011.

[46] C. J. Barelle, E. A. Bohula, S. J. Kron, D. Wessels, D. R. Soll, A. Schäfer, A. J. P. Brown, and N. A. R. Gow. Asynchronous cell cycle and asymmetric vacuolar inheritance in true hyphae of *Candida albicans*. *Eukaryotic cell*, 2(3):398–410, 2003.

bioRxiv preprint doi: https://doi.org/10.1101/041509; this version posted February 26, 2016. The copyright holder for this preprint (which was not certified by peer review) is the author/funder. All rights reserved. No reuse allowed without permission.

Appendix A: GM2

Diagonal component

It is simpler to derive the pairwise density functions for GM2 for a domain of size $(N_x+1)\times(N_y+1)$ (this avoids having (N_x-1) in the denominator of a number of fractions). For GM2 it is also necessary to introduce some new notation. The distance of the lattice site $\mathbf{m}$ from the boundary (origin of growth) is m_i and m_j, i.e. the position of $\mathbf{m}$, and the distance of the lattice site $\mathbf{n}$ from boundary, n_i and n_j, i.e. the position of $\mathbf{m}+(r_x,r_y)$. The evolution of the pairwise density functions for the diagonal component of GM2 is

$$
\begin{aligned}
\sum_{i=1}^{N_x+1}\sum_{j=1}^{N_y+1}\rho^{(N_x+1)\times(N_y+1)}(\mathbf{m},\mathbf{m}+(r_x,r_y);t+\delta t) = \\
&(1-\delta t P_{g_x}(N_x+1)-\delta t P_{g_y}(N_y+1))\sum_{i=1}^{N_x+1}\sum_{j=1}^{N_y+1}\rho^{(N_x+1)\times(N_y+1)}(\mathbf{m},\mathbf{m}+(r_x,r_y);t)\\
&+\delta t P_{g_y}(N_y)\sum_{i=1}^{N_x+1}\sum_{j=1}^{N_y}\left(\frac{m_j n_j}{(N_y)(N_y)}\right)\rho^{(N_x+1)\times N_y}(\mathbf{m},\mathbf{m}+(r_x,r_y);t)\\
&+\delta t P_{g_y}(N_y)\sum_{i=1}^{N_x+1}\sum_{j=1}^{N_y}\left(\frac{(N_y-m_j)(N_y-n_j)}{(N_y)(N_y)}\right)\rho^{(N_x+1)\times N_y}(\mathbf{m},\mathbf{m}+(r_x,r_y);t)\\
&+\delta t P_{g_y}(N_y)\sum_{i=1}^{N_x+1}\sum_{j=1}^{N_y}\left(\frac{(N_y-m_j)(n_j-1)}{(N_y)(N_y)}\right)\rho^{(N_x+1)\times N_y}(\mathbf{m},\mathbf{m}+(r_x,r_y-1);t)\\
&+\delta t P_{g_y}(N_y)\sum_{i=1}^{N_x+1}\sum_{j=1}^{N_y}\left(\frac{(m_j-1)(N_y-n_j)}{(N_y)(N_y)}\right)\rho^{(N_x+1)\times N_y}(\mathbf{m},\mathbf{m}+(r_x,r_y+1);t)\\
&+\delta t P_{g_x}(N_x)\sum_{i=1}^{N_x}\sum_{j=1}^{N_y+1}\left(\frac{m_i n_i}{(N_x)(N_x)}\right)\rho^{N_x\times(N_y+1)}(\mathbf{m},\mathbf{m}+(r_x,r_y);t)\\
&+\delta t P_{g_x}(N_x)\sum_{i=1}^{N_x}\sum_{j=1}^{N_y+1}\left(\frac{(N_x-m_i)(N_x-n_i)}{(N_x)(N_x)}\right)\rho^{N_x\times(N_y+1)}(\mathbf{m},\mathbf{m}+(r_x,r_y);t)\\
&+\delta t P_{g_x}(N_x)\sum_{i=1}^{N_x}\sum_{j=1}^{N_y+1}\left(\frac{(N_x-m_i)(n_i-1)}{(N_x)(N_x)}\right)\rho^{N_x\times(N_y+1)}(\mathbf{m},\mathbf{m}+(r_x-1,r_y);t)\\
&+\delta t P_{g_x}(N_x)\sum_{i=1}^{N_x}\sum_{j=1}^{N_y+1}\left(\frac{(m_i-1)(N_x-n_i)}{(N_x)(N_x)}\right)\rho^{N_x\times(N_y+1)}(\mathbf{m},\mathbf{m}+(r_x+1,r_y);t). \qquad (36)
\end{aligned}
$$

bioRxiv preprint doi: https://doi.org/10.1101/041509; this version posted February 26, 2016. The copyright holder for this preprint (which was not certified by peer review) is the author/funder. All rights reserved. No reuse allowed without permission.

The terms on the RHS of Eq. (36) represent: i) the sum of pairwise density functions a distance (r_x, r_y) apart on a domain of size $(N_x+1)(N_y+1)$ multiplied by the probability that no growth occurs in $[t+\delta t)$, ii) the sum of pairwise density functions a distance (r_x, r_y) apart on a domain of size $(N_x+1)(N_y)$ multiplied by the probability that a growth event occurs in the vertical direction and both agents are moved by it, iii) the sum of pairwise density functions a distance (r_x, r_y) apart on a domain of size $(N_x+1)(N_y)$ multiplied by the probability that a growth event occurs in the vertical direction and both agents are not moved by it, iv) the sum of pairwise density functions a distance (r_x, r_y-1) apart on a domain of size $(N_x+1)(N_y)$ multiplied by the probability that a growth event occurs in the vertical direction and $\mathbf{m}+(r_x, r_y)$ moves and $\mathbf{m}$ does not move (we can write this in terms of a displacement vector: (r_x, r_y-1)), and v) the sum of pairwise density functions a distance (r_x, r_y+1) apart on a domain of size $(N_x+1)(N_y)$ multiplied by the probability that a growth event occurs in the vertical direction and $\mathbf{m}$ moves and $\mathbf{m}+(r_x, r_y)$ does not move. The rest of the terms are the equivalent for growth in the horizontal direction. First, we assume translational invariance and simplify Eq. (36) to obtain

$$\begin{aligned}
\sum_{i=1}^{N_x+1}\sum_{j=1}^{N_y+1} \rho^{(N_x+1)\times(N_y+1)}(r_x, r_y; t+\delta t) = \\
&(1-\delta t P_{g_x}(N_x+1) - \delta t P_{g_y}(N_y+1)) \sum_{i=1}^{N_x+1}\sum_{j=1}^{N_y+1} \rho^{(N_x+1)\times(N_y+1)}(r_x, r_y; t) \\
&+ \delta t P_{g_y} \sum_{i=1}^{N_x+1}\sum_{j=1}^{N_y} \left(N_y - n_j - m_j + \frac{2m_j n_j}{N_y}\right) \rho^{(N_x+1)\times N_y}(r_x, r_y; t) \\
&+ \delta t P_{g_y} \sum_{i=1}^{N_x+1}\sum_{j=1}^{N_y} \left(\frac{(N_y - m_j)(n_j - 1)}{(N_y)}\right) \rho^{(N_x+1)\times N_y}(r_x, r_y - 1; t) \\
&+ \delta t P_{g_y} \sum_{i=1}^{N_x+1}\sum_{j=1}^{N_y} \left(\frac{(m_j - 1)(N_y - n_j)}{(N_y)}\right) \rho^{(N_x+1)\times N_y}(r_x, r_y + 1; t) \\
&+ \delta t P_{g_x} \sum_{i=1}^{N_x}\sum_{j=1}^{N_y+1} \left(N_x - n_i - m_i + \frac{2m_i n_i}{N_x}\right) \rho^{N_x\times(N_y+1)}(r_x, r_y; t) \\
&+ \delta t P_{g_x} \sum_{i=1}^{N_x}\sum_{j=1}^{N_y+1} \left(\frac{(N_x - m_i)(n_i - 1)}{(N_x)}\right) \rho^{N_x\times(N_y+1)}(r_x - 1, r_y; t) \\
&+ \delta t P_{g_x} \sum_{i=1}^{N_x}\sum_{j=1}^{N_y+1} \left(\frac{(m_i - 1)(N_x - n_i)}{(N_x)}\right) \rho^{N_x\times(N_y+1)}(r_x + 1, r_y; t). \qquad (37)
\end{aligned}$$

bioRxiv preprint doi: https://doi.org/10.1101/041509; this version posted February 26, 2016. The copyright holder for this preprint (which was not certified by peer review) is the author/funder. All rights reserved. No reuse allowed without permission.

We rewrite Eq. (37) using $\tilde{n}_x$, $\tilde{m}_x$ and $\tilde{m_x n_x}$, which are constants defined as

$$\tilde{n}_x = \frac{1}{(N_x)(N_y+1)} \sum_{i=1}^{N_x} \sum_{j=1}^{N_y+1} n_i, \tag{38}$$

and

$$\tilde{m}_x = \frac{1}{(N_x)(N_y+1)} \sum_{i=1}^{N_x} \sum_{j=1}^{N_y+1} m_i, \tag{39}$$

and

$$\begin{aligned}
\tilde{m_x n_x} = & \frac{1}{(N_x)(N_y+1)} \sum_{i=1}^{N_x} \sum_{j=1}^{N_y+1} m_i n_i = \\
& \frac{1}{(N_x)(N_y+1)} \sum_{j=1}^{N_y+1} \left[\sum_{i=1}^{N_x-r_x} (m_i)(m_i+r_x) + \sum_{i=N_x-r_x+1}^{N_x} (m_i)(m_i-(N_x-r_x)) \right] \\
& \frac{1}{(N_x)(N_y+1)} \sum_{j=1}^{N_y+1} \left[\sum_{i=1}^{N_x} (m_i)(m_i+r_x) - \sum_{i=N_x-r_x+1}^{N_x} N_x m_i \right] \\
& \frac{1}{(N_x)(N_y+1)} \sum_{j=1}^{N_y+1} \left[\sum_{i=1}^{N_x} (m_i)(m_i+r_x) + N_x \left(\sum_{i=1}^{N_x-r_x} m_i - \sum_{i=1}^{N_x} m_i \right) \right].
\end{aligned} \tag{40}$$

Eqs. (38)-(40) can be evaluated directly. If we do so we obtain:

$$\tilde{n}_x = \frac{(N_x+1)}{2}; \tag{41}$$

$$\tilde{m}_x = \frac{(N_x+1)}{2}; \tag{42}$$

and

$$\tilde{m_x n_x} = N_x \left(\frac{N_x}{3} + \frac{1}{2} \right) + \frac{r_x}{2} (r_x - N_x) + \frac{1}{6}. \tag{43}$$

It is important to note that if in Eq. (43) we set $r_x = 0$, for instance for colinear lattice sites,

bioRxiv preprint doi: https://doi.org/10.1101/041509; this version posted February 26, 2016. The copyright holder for this preprint (which was not certified by peer review) is the author/funder. All rights reserved. No reuse allowed without permission.

we obtain

$$m_x\tilde{n}_x = N_x\left(\frac{N_x}{3}+\frac{1}{2}\right)+\frac{1}{6}. \tag{44}$$

However, initially we substitute Eqs. (38)-(40) into Eq. (37) to obtain

bioRxiv preprint doi: https://doi.org/10.1101/041509; this version posted February 26, 2016. The copyright holder for this preprint (which was not certified by peer review) is the author/funder. All rights reserved. No reuse allowed without permission.

$$
\begin{aligned}
(N_x+1)(N_y+1)\rho^{(N_x+1)\times(N_y+1)}(r_x,r_y;t+\delta t) = {} & (1-\delta t P_{g_x}(N_x+1)-\delta t P_{g_y}(N_y+1))(N_x+1)(N_y+1)\rho^{(N_x+1)\times(N_y+1)}(r_x,r_y;t) \\
& + \delta t P_{g_y}(N_x+1)(N_y)\left(N_y-\tilde{n}_y-\tilde{m}_y+\frac{2\tilde{m_y}n_y}{N_y}\right)\rho^{(N_x+1)\times N_y}(r_x,r_y;t) \\
& + \delta t P_{g_y}(N_x+1)(N_y)\left(\tilde{n}_y-1-\frac{\tilde{m_y}n_y}{N_y}+\frac{\tilde{m}_y}{N_y}\right)\rho^{(N_x+1)\times N_y}(r_x,r_y-1;t) \\
& + \delta t P_{g_y}(N_x+1)(N_y)\left(\tilde{m}_y-1-\frac{\tilde{m_y}n_y}{N_y}+\frac{\tilde{n}_y}{N_y}\right)\rho^{(N_x+1)\times N_y}(r_x,r_y+1;t) \\
& + \delta t P_{g_x}(N_x)(N_y+1)\left(N_x-\tilde{n}_x-\tilde{m}_x+\frac{2\tilde{m_x}n_x}{N_x}\right)\rho^{N_x\times(N_y+1)}(r_x,r_y;t) \\
& + \delta t P_{g_x}(N_x)(N_y+1)\left(\tilde{n}_x-1-\frac{\tilde{m_x}n_x}{N_x}+\frac{\tilde{m}_x}{N_x}\right)\rho^{N_x\times(N_y+1)}(r_x-1,r_y;t) \\
& + \delta t P_{g_x}(N_x)(N_y+1)\left(\tilde{m}_x-1-\frac{\tilde{m_x}n_x}{N_x}+\frac{\tilde{n}_x}{N_x}\right)\rho^{N_x\times(N_y+1)}(r_x+1,r_y;t). \qquad (45)
\end{aligned}
$$

That Eqs. (37) and (45) are equivalent can be shown by substituting Eqs. (38)-(40) into Eq. (45).

bioRxiv preprint doi: https://doi.org/10.1101/041509; this version posted February 26, 2016. The copyright holder for this preprint (which was not certified by peer review) is the author/funder. All rights reserved. No reuse allowed without permission.

If we now apply the approximation,

$$\rho^{(N_x+1)\times(N_y+1)}(r_x, r_y; t) \approx \left(\frac{N_y}{N_y+1}\right)\rho^{(N_x+1)\times N_y}(r_x, r_y; t), \tag{46}$$

to Eq. (45) we obtain

$$\begin{aligned}
\rho^{(N_x+1)\times(N_y+1)}(r_x, r_y; t+\delta t) = \\
&(1-\delta t P_{g_x}(N_x+1) - \delta t P_{g_y}(N_y+1))\rho^{(N_x+1)\times(N_y+1)}(r_x, r_y; t) \\
&+ \delta t P_{g_y}\left(N_y - \tilde{n}_y - \tilde{m}_y + \frac{2\tilde{m_y}n_y}{N_y}\right)\rho^{(N_x+1)\times(N_y+1)}(r_x, r_y; t) \\
&+ \delta t P_{g_y}\left(\tilde{n}_y - 1 - \frac{\tilde{m_y}n_y}{N_y} + \frac{\tilde{m}_y}{N_y}\right)\rho^{(N_x+1)\times(N_y+1)}(r_x, r_y-1; t) \\
&+ \delta t P_{g_y}\left(\tilde{m}_y - 1 - \frac{\tilde{m_y}n_y}{N_y} + \frac{\tilde{n}_y}{N_y}\right)\rho^{(N_x+1)\times(N_y+1)}(r_x, r_y+1; t) \\
&+ \delta t P_{g_x}\left(N_x - \tilde{n}_x - \tilde{m}_x + \frac{2\tilde{m_x}n_x}{N_x}\right)\rho^{(N_x+1)\times(N_y+1)}(r_x, r_y; t) \\
&+ \delta t P_{g_x}\left(\tilde{n}_x - 1 - \frac{\tilde{m_x}n_x}{N_x} + \frac{\tilde{m}_x}{N_x}\right)\rho^{(N_x+1)\times(N_y+1)}(r_x-1, r_y; t) \\
&+ \delta t P_{g_x}\left(\tilde{m}_x - 1 - \frac{\tilde{m_x}n_x}{N_x} + \frac{\tilde{n}_x}{N_x}\right)\rho^{(N_x+1)\times(N_y+1)}(r_x+1, r_y; t).
\end{aligned} \tag{47}$$

If we rearrange Eq. (47) and take the limit as $\delta t \to 0$ we obtain

$$\begin{aligned}
\frac{\mathrm{d}\rho_2^{(N_x+1)\times(N_y+1)}(r_x, r_y; t+\delta t)}{\mathrm{d}t} = &-(P_{g_x}(N_x+1) + P_{g_y}(N_y+1))\rho_2^{(N_x+1)\times(N_y+1)}(r_x, r_y; t) \\
&+ P_{g_y}\left(N_y - \tilde{n}_y - \tilde{m}_y + \frac{2\tilde{m_y}n_y}{N_y}\right)\rho_2^{(N_x+1)\times(N_y+1)}(r_x, r_y; t) \\
&+ P_{g_y}\left(\tilde{n}_y - 1 - \frac{\tilde{m_y}n_y}{N_y} + \frac{\tilde{m}_y}{N_y}\right)\rho_2^{(N_x+1)\times(N_y+1)}(r_x, r_y-1; t) \\
&+ P_{g_y}\left(\tilde{m}_y - 1 - \frac{\tilde{m_y}n_y}{N_y} + \frac{\tilde{n}_y}{N_y}\right)\rho_2^{(N_x+1)\times(N_y+1)}(r_x, r_y+1; t) \\
&+ P_{g_x}\left(N_x - \tilde{n}_x - \tilde{m}_x + \frac{2\tilde{m_x}n_x}{N_x}\right)\rho_2^{(N_x+1)\times(N_y+1)}(r_x, r_y; t) \\
&+ P_{g_x}\left(\tilde{n}_x - 1 - \frac{\tilde{m_x}n_x}{N_x} + \frac{\tilde{m}_x}{N_x}\right)\rho_2^{(N_x+1)\times(N_y+1)}(r_x-1, r_y; t) \\
&+ P_{g_x}\left(\tilde{m}_x - 1 - \frac{\tilde{m_x}n_x}{N_x} + \frac{\tilde{n}_x}{N_x}\right)\rho_2^{(N_x+1)\times(N_y+1)}(r_x+1, r_y; t),
\end{aligned} \tag{48}$$

bioRxiv preprint doi: https://doi.org/10.1101/041509; this version posted February 26, 2016. The copyright holder for this preprint (which was not certified by peer review) is the author/funder. All rights reserved. No reuse allowed without permission.

which we can simplify further to obtain

$$\begin{aligned}\frac{\mathrm{d}\rho^{(N_x+1)\times(N_y+1)}(r_x,r_y;t+\delta t)}{\mathrm{d}t} &= P_{g_x}\left(-1+\left(\frac{2m_x\tilde{n}_x}{N_x}\right)-\tilde{n}_x-\tilde{m}_x\right)\rho^{(N_x+1)\times(N_y+1)}(r_x,r_y;t)\\ &+P_{g_y}\left(-1+\left(\frac{2m_y\tilde{n}_y}{N_y}\right)-\tilde{n}_y-\tilde{m}_y\right)\rho^{(N_x+1)\times(N_y+1)}(r_x,r_y;t)\\ &+P_{g_y}\left(\tilde{n}_y-1-\frac{m_y\tilde{n}_y}{N_y}+\frac{\tilde{m}_y}{N_y}\right)\rho^{(N_x+1)\times(N_y+1)}(r_x,r_y-1;t)\\ &+P_{g_y}\left(\tilde{m}_y-1-\frac{m_y\tilde{n}_y}{N_y}+\frac{\tilde{n}_y}{N_y}\right)\rho^{(N_x+1)\times(N_y+1)}(r_x,r_y+1;t)\\ &+P_{g_x}\left(\tilde{n}_x-1-\frac{m_x\tilde{n}_x}{N_x}+\frac{\tilde{m}_x}{N_x}\right)\rho^{(N_x+1)\times(N_y+1)}(r_x-1,r_y;t)\\ &+P_{g_x}\left(\tilde{m}_x-1-\frac{m_x\tilde{n}_x}{N_x}+\frac{\tilde{n}_x}{N_x}\right)\rho^{(N_x+1)\times(N_y+1)}(r_x+1,r_y;t). \end{aligned} \tag{49}$$

If we now evaluate Eqs. (38)-(40) with Eqs. (41)-(43) we obtain

$$\frac{\mathrm{d}\rho_2^{(N_x+1)\times(N_y+1)}(r_x,r_y;t+\delta t)}{\mathrm{d}t} = \tag{50}$$

$$\begin{aligned}&P_{g_x}\left(-1-\frac{N_x}{3}+r_x\left(\frac{r_x}{N_x}-1\right)+\frac{1}{3N_x}\right)\rho_2^{(N_x+1)\times(N_y+1)}(r_x,r_y;t)\\ &+P_{g_y}\left(-1-\frac{N_y}{3}+r_y\left(\frac{r_y}{N_y}-1\right)+\frac{1}{3N_y}\right)\rho_2^{(N_x+1)\times(N_y+1)}(r_x,r_y;t)\\ &+P_{g_y}\left(-\frac{1}{2}+\frac{N_y}{6}-\frac{r_y}{2}\left(\frac{r_y}{N_y}-1\right)-\frac{1}{3N_y}\right)\rho_2^{(N_x+1)\times(N_y+1)}(r_x,r_y-1;t)\\ &+P_{g_y}\left(-\frac{1}{2}+\frac{N_y}{6}-\frac{r_y}{2}\left(\frac{r_y}{N_y}-1\right)-\frac{1}{3N_y}\right)\rho_2^{(N_x+1)\times(N_y+1)}(r_x,r_y+1;t)\\ &+P_{g_x}\left(-\frac{1}{2}+\frac{N_x}{6}-\frac{r_x}{2}\left(\frac{r_x}{N_x}-1\right)-\frac{1}{3N_x}\right)\rho_2^{(N_x+1)\times(N_y+1)}(r_x-1,r_y;t)\\ &+P_{g_x}\left(-\frac{1}{2}+\frac{N_x}{6}-\frac{r_x}{2}\left(\frac{r_x}{N_x}-1\right)-\frac{1}{3N_x}\right)\rho_2^{(N_x+1)\times(N_y+1)}(r_x+1,r_y;t). \end{aligned} \tag{51}$$

This is Eq. (22) of the main text.

bioRxiv preprint doi: https://doi.org/10.1101/041509; this version posted February 26, 2016. The copyright holder for this preprint (which was not certified by peer review) is the author/funder. All rights reserved. No reuse allowed without permission.

Colinear component

For the colinear component we have (assuming that lattice sites are horizontally colinear, i.e. $r_y = 0$)

$$\begin{aligned}
\sum_{i=1}^{N_x+1}\sum_{j=1}^{N_y+1} \rho_2^{(N_x+1)\times(N_y+1)}(\mathbf{m},\mathbf{m}+(r_x,0);t+\delta t) = \\
&(1-\delta t P_{g_x}(N_x+1)-\delta t P_{g_y}(N_y+1))\sum_{i=1}^{N_x+1}\sum_{j=1}^{N_y+1}\rho_2^{(N_x+1)\times(N_y+1)}(\mathbf{m},\mathbf{m}+(r_x,0);t)\\
&+\delta t P_{g_y}\sum_{i=1}^{N_x+1}\sum_{j=1}^{N_y}\left(\frac{m_j n_j}{N_y}\right)\rho_2^{(N_x+1)\times N_y}(\mathbf{m},\mathbf{m}+(r_x,r_y);t)\\
&+\delta t P_{g_y}\sum_{i=1}^{N_x+1}\sum_{j=1}^{N_y}\left(N_y-n_j-m_j+\frac{m_j n_j}{N_y}\right)\rho_2^{(N_x+1)\times N_y}(\mathbf{m},\mathbf{m}+(r_x,0);t)\\
&+\delta t P_{g_y}\sum_{i=1}^{N_x+1}\sum_{j=1}^{N_y}\left(n_j-1-\frac{m_j n_j}{N_y}+\frac{m_j}{N_y}\right)\rho_2^{(N_x+1)\times N_y}(\mathbf{m},\mathbf{m}+(r_x,-1);t)\\
&+\delta t P_{g_y}\sum_{i=1}^{N_x+1}\sum_{j=1}^{N_y}\left(m_j-1-\frac{m_j n_j}{N_y}+\frac{n_j}{N_y}\right)\rho_2^{(N_x+1)\times N_y}(\mathbf{m},\mathbf{m}+(r_x,-1);t)\\
&+\delta t P_{g_x}\sum_{i=1}^{N_x}\sum_{j=1}^{N_y+1}(r_x-1)\rho_2^{N_x\times(N_y+1)}(\mathbf{m},\mathbf{m}+(r_x-1,0);t)\\
&+\delta t P_{g_x}\sum_{i=1}^{N_x}\sum_{j=1}^{N_y+1}(N_x-r_x)\rho_2^{N_x\times(N_y+1)}(\mathbf{m},\mathbf{m}+(r_x,0);t). \qquad (52)
\end{aligned}$$

bioRxiv preprint doi: https://doi.org/10.1101/041509; this version posted February 26, 2016. The copyright holder for this preprint (which was not certified by peer review) is the author/funder. All rights reserved. No reuse allowed without permission.

We rewrite Eq. (52) using Eqs. (38)-(40) to obtain

$$
\begin{aligned}
(N_x+1)(N_y+1)\rho_2^{(N_x+1)\times(N_y+1)}(r_x,0;t+\delta t) = \\
&(1-\delta t P_{g_x}(N_x+1)-\delta t P_{g_y}(N_y+1))(N_x+1)(N_y+1)\rho_2^{(N_x+1)\times(N_y+1)}(r_x,0;t) \\
&+\delta t P_{g_y}(N_x+1)(N_y)\left(\frac{m_{\tilde{y}}n_y}{N_y}\right)\rho_2^{(N_x+1)\times N_y}(r_x,0;t) \\
&+\delta t P_{g_y}(N_x+1)(N_y)\left(N_y-\tilde{n}_y-\tilde{m}_y+\frac{m_{\tilde{y}}n_y}{N_y}\right)\rho_2^{(N_x+1)\times N_y}(r_x,0;t) \\
&+\delta t P_{g_y}(N_x+1)(N_y)\left(\tilde{n}_y-1-\frac{m_{\tilde{y}}n_y}{N_y}+\frac{\tilde{m}_y}{N_y}\right)\rho_2^{(N_x+1)\times N_y}(r_x,-1;t) \\
&+\delta t P_{g_y}(N_x+1)(N_y)\left(\tilde{m}_y-1-\frac{m_{\tilde{y}}n_y}{N_y}+\frac{\tilde{n}_y}{N_y}\right)\rho_2^{(N_x+1)\times N_y}(r_x,-1;t) \\
&+\delta t P_{g_x}(N_x)(N_y+1)(r_x-1)\rho_2^{N_x\times(N_y+1)}(r_x-1,0;t) \\
&+\delta t P_{g_x}(N_x)(N_y+1)(N_x-r_x)\rho_2^{N_x\times(N_y+1)}(r_x,0;t). \qquad (53)
\end{aligned}
$$

bioRxiv preprint doi: https://doi.org/10.1101/041509; this version posted February 26, 2016. The copyright holder for this preprint (which was not certified by peer review) is the author/funder. All rights reserved. No reuse allowed without permission.

We now make the approximation Eq. (46) to obtain

$$\begin{aligned}\rho_2^{(N_x+1)\times(N_y+1)}(r_x,0;t+\delta t) &= (1-\delta t P_{g_x}(N_x+1)-\delta t P_{g_y}(N_y+1))\rho_2^{(N_x+1)\times(N_y+1)}(r_x,0;t)\\ &+\delta t P_{g_y}\left(\frac{m_y\tilde{n}_y}{N_y}\right)\rho_2^{(N_x+1)\times(N_y+1)}(r_x,0;t)\\ &+\delta t P_{g_y}\left(N_y-\tilde{n}_y-\tilde{m}_y+\frac{m_y\tilde{n}_y}{N_y}\right)\rho_2^{(N_x+1)\times(N_y+1)}(r_x,0;t)\\ &+\delta t P_{g_y}\left(\tilde{n}_y-1-\frac{m_y\tilde{n}_y}{N_y}+\frac{\tilde{m}_y}{N_y}\right)\rho_2^{(N_x+1)\times(N_y+1)}(r_x,-1;t)\\ &+\delta t P_{g_y}\left(\tilde{m}_y-1-\frac{m_y\tilde{n}_y}{N_y}+\frac{\tilde{n}_y}{N_y}\right)\rho_2^{(N_x+1)\times(N_y+1)}(r_x,-1;t)\\ &+\delta t P_{g_x}(r_x-1)\rho_2^{(N_x+1)\times(N_y+1)}(r_x-1,0;t)\\ &+\delta t P_{g_x}(N_x-r_x)\rho_2^{(N_x+1)\times(N_y+1)}(r_x,0;t),\end{aligned} \tag{54}$$

which we can simplify to obtain

$$\begin{aligned}\frac{\mathrm{d}\rho_2^{(N_x+1)\times(N_y+1)}(r_x,0;t)}{\mathrm{d}t} &= -P_{g_x}(r_x+1)\rho_2^{(N_x+1)\times(N_y+1)}(r_x,0;t)\\ &+P_{g_x}(r_x-1)\rho_2^{(N_x+1)\times(N_y+1)}(r_x-1,0;t)\\ &+P_{g_y}\left(-(N_y+1)+\left(\frac{2m_y\tilde{n}_y}{N_y}\right)+N_y-\tilde{n}_y-\tilde{m}_y\right)\rho_2^{(N_x+1)\times(N_y+1)}(r_x,0;t)\\ &+P_{g_y}\left(\tilde{n}_y-1-\frac{m_y\tilde{n}_y}{N_y}+\frac{\tilde{m}_y}{N_y}\right)\rho_2^{(N_x+1)\times(N_y+1)}(r_x,-1;t)\\ &+P_{g_y}\left(\tilde{m}_y-1-\frac{m_y\tilde{n}_y}{N_y}+\frac{\tilde{n}_y}{N_y}\right)\rho_2^{(N_x+1)\times(N_y+1)}(r_x,-1;t).\end{aligned} \tag{55}$$

If we evaluate Eqs. (38)-(40) with (41)-(43) we obtain

$$\begin{aligned}\frac{\mathrm{d}\rho_2^{(N_x+1)\times(N_y+1)}(r_x,0;t)}{\mathrm{d}t} &= -P_{g_x}(r_x+1)\rho_2^{(N_x+1)\times(N_y+1)}(r_x,0;t)\\ &+P_{g_x}(r_x-1)\rho_2^{(N_x+1)\times(N_y+1)}(r_x-1,0;t)\\ &+P_{g_y}\left(-1-\frac{N_y}{3}+\frac{1}{3N_y}\right)\rho_2^{(N_x+1)\times(N_y+1)}(r_x,0;t)\\ &+P_{g_y}\left(-1+\frac{N_y}{3}+\frac{2}{3N_y}\right)\rho_2^{(N_x+1)\times(N_y+1)}(r_x,-1;t).\end{aligned} \tag{56}$$

This is Eq. (21).

bioRxiv preprint doi: https://doi.org/10.1101/041509; this version posted February 26, 2016. The copyright holder for this preprint (which was not certified by peer review) is the author/funder. All rights reserved. No reuse allowed without permission.

Appendix B

We display how to include agent proliferation and motility in the individual density functions. To do so we require to introduce further notation. We indicate a site unoccupied by an agent in the following manner, $\rho_1^{N_x \times N_y}(\mathbf{m}'; t)$, that is, the joint probability of lattice site $\mathbf{m}$ not being occupied on a domain of size $N_x \times N_y$ at time t. We also introduce the summation,

$$\sum_{\mathbf{n}}^{\mathbf{m}} \rho_2^{N_x \times N_y}(\mathbf{m}, \mathbf{n}; t) = \rho_2^{N_x \times N_y}((i,j),(i+1,j);t) + \rho_2^{N_x \times N_y}((i,j),(i-1,j);t) + \rho_2^{N_x \times N_y}((i,j),(i,j+1);t) + \rho_2^{N_x \times N_y}((i,j),(i,j-1);t). \tag{57}$$

which indexes over the von Neumann neighbourhood of the site indicated as the upper index.

The sum of the individual density functions on a domain of size $N_x \times N_y$ at $[t + \delta t)$ for motile and proliferating agents is

$$\begin{aligned}\sum_{i=1}^{N_x}\sum_{j=1}^{N_y} \rho_1^{N_x \times N_y}(\mathbf{m}; t+\delta t) = {} & (1 - \delta t P_{g_x} N_x - \delta t P_{g_y} N_y) \sum_{i=1}^{N_x}\sum_{j=1}^{N_y} \rho_1^{N_x \times N_y}(\mathbf{m}; t) \\ & + \delta t P_{g_x} \sum_{i=1}^{N_x-1}\sum_{j=1}^{N_y} (N_x - 1)\rho_1^{(N_x-1)\times N_y}(\mathbf{m}; t) \\ & + \delta t P_{g_y} \sum_{i=1}^{N_x}\sum_{j=1}^{N_y-1} (N_y - 1)\rho_1^{N_x \times (N_y-1)}(\mathbf{m}; t) \\ & + \delta t \frac{P_m}{4} \sum_{i=1}^{N_x}\sum_{j=1}^{N_y} \left[\sum_{\mathbf{n}}^{\mathbf{m}} \left[\rho_2^{N_x \times N_y}(\mathbf{m}', \mathbf{n}; t) - \rho_2^{N_x \times N_y}(\mathbf{m}, \mathbf{n}'; t) \right] \right] \\ & + \delta t \frac{P_p}{4} \sum_{i=1}^{N_x}\sum_{j=1}^{N_y} \left[\sum_{\mathbf{n}}^{\mathbf{m}} \left[\rho_2^{N_x \times N_y}(\mathbf{m}', \mathbf{n}; t) \right] \right] + \mathcal{O}(\delta t^2).\end{aligned} \tag{58}$$

bioRxiv preprint doi: https://doi.org/10.1101/041509; this version posted February 26, 2016. The copyright holder for this preprint (which was not certified by peer review) is the author/funder. All rights reserved. No reuse allowed without permission.

As we assume translational invariance Eq. (58) can be simplified to obtain

$$\begin{aligned}\sum_{i=1}^{N_x}\sum_{j=1}^{N_y}\rho_1^{N_x\times N_y}(\mathbf{m};t+\delta t) &= (1-\delta t P_{g_x}N_x-\delta t P_{g_y}N_y)\sum_{i=1}^{N_x}\sum_{j=1}^{N_y}\rho_1^{N_x\times N_y}(\mathbf{m};t)\\ &+\delta t P_{g_x}\sum_{i=1}^{N_x-1}\sum_{j=1}^{N_y}(N_x-1)\rho_1^{(N_x-1)\times N_y}(\mathbf{m};t)\\ &+\delta t P_{g_y}\sum_{i=1}^{N_x}\sum_{j=1}^{N_y-1}(N_y-1)\rho_1^{N_x\times(N_y-1)}(\mathbf{m};t)\\ &+\delta t\frac{P_p}{4}\sum_{i=1}^{N_x}\sum_{j=1}^{N_y}\left[\sum_{\mathbf{n}}^{\mathbf{m}}\rho_2^{N_x\times N_y}(\mathbf{m}',\mathbf{n};t)\right]+\mathcal{O}(\delta t^2). \qquad (59)\end{aligned}$$

If we recognise that $\rho_2^{N_x\times N_y}(\mathbf{m}',\mathbf{n};t)=\rho_1^{N_x\times N_y}(\mathbf{m};t)-\rho_2^{N_x\times N_y}(1,0;t)$ we can rewrite Eq. (59) as

$$\begin{aligned}\sum_{i=1}^{N_x}\sum_{j=1}^{N_y}\rho_1^{N_x\times N_y}(\mathbf{m};t+\delta t) &= (1-\delta t P_{g_x}N_x-\delta t P_{g_y}N_y)\sum_{i=1}^{N_x}\sum_{j=1}^{N_y}\rho_1^{N_x\times N_y}(\mathbf{m};t)\\ &+\delta t P_{g_x}\sum_{i=1}^{N_x-1}\sum_{j=1}^{N_y}(N_x-1)\rho_1^{(N_x-1)\times N_y}(\mathbf{m};t)\\ &+\delta t P_{g_y}\sum_{i=1}^{N_x}\sum_{j=1}^{N_y-1}(N_y-1)\rho_1^{N_x\times(N_y-1)}(\mathbf{m};t)\\ &+\delta t P_p\sum_{i=1}^{N_x}\sum_{j=1}^{N_y}\left[\rho_1^{N_x\times N_y}(\mathbf{m};t)-\rho_2^{N_x\times N_y}(1,0;t)\right]+\mathcal{O}(\delta t^2). \qquad (60)\end{aligned}$$

From Eq. (60) we can obtain

$$\frac{\mathrm{d}c(t)}{\mathrm{d}t}=-(P_{g_x}+P_{g_y})c(t)+P_p(c(t)-\rho_2^{N_x\times N_y}(1,0;t)), \qquad (61)$$

which is Eq. (26).

The derivation of the pairwise density functions can be found in [25], and the equations are stated in the supplementary material of [25]. However, we also outline the derivation below. The addition of agent motility and proliferation is the same for GM1 and GM2. For agents colinear in the horizontal direction, that is, r_y is zero, and $r_x>1$, the evolution of the pairwise

bioRxiv preprint doi: https://doi.org/10.1101/041509; this version posted February 26, 2016. The copyright holder for this preprint (which was not certified by peer review) is the author/funder. All rights reserved. No reuse allowed without permission.

density functions for motile and proliferative agents with GM1 is

$$
\begin{aligned}
\sum_{i=1}^{N_x}\sum_{j=1}^{N_y}\rho_2^{N_x\times N_y}(r_x,0;t+\delta t) = \\
&(1-\delta t P_{g_x}N_x-\delta t P_{g_y}N_y)\sum_{i=1}^{N_x}\sum_{j=1}^{N_y}\rho_2^{N_x\times N_y}(r_x,0;t)\\
&+\delta t P_{g_x}\sum_{i=1}^{N_x-1}\sum_{j=1}^{N_y}(r_x-1)\rho_2^{(N_x-1)\times N_y}(r_x-1,0;t)\\
&+\delta t P_{g_x}\sum_{i=1}^{N_x-1}\sum_{j=1}^{N_y}(N_x-1-r_x)\rho_2^{(N_x-1)\times N_y}(r_x,0;t)\\
&+\delta t P_{g_y}\sum_{i=1}^{N_x}\sum_{j=1}^{N_y-1}(N_y-1)\rho_2^{N_x\times(N_y-1)}(r_x,0;t)\\
&+\delta t\frac{P_m}{4}\sum_{i=1}^{N_x}\sum_{j=1}^{N_y}\Bigg[\sum_{\mathbf{k}}^{\mathbf{n}}\left[\rho_3^{N_x\times N_y}(\mathbf{m},\mathbf{n}',\mathbf{k};t)-\rho_3^{N_x\times N_y}(\mathbf{m},\mathbf{n},\mathbf{k}';t)\right]\\
&+\sum_{\mathbf{k}}^{\mathbf{m}}\left[\rho_3^{N_x\times N_y}(\mathbf{m}',\mathbf{n},\mathbf{k};t)-\rho_3^{N_x\times N_y}(\mathbf{m},\mathbf{n},\mathbf{k}';t)\right]\Bigg]\\
&+\delta t\frac{P_p}{4}\sum_{i=1}^{N_x}\sum_{j=1}^{N_y}\left[\sum_{\mathbf{k}}^{\mathbf{m}}\left[\rho_3^{N_x\times N_y}(\mathbf{m}',\mathbf{n},\mathbf{k};t)\right]+\sum_{\mathbf{k}}^{\mathbf{n}}\left[\rho_3^{N_x\times N_y}(\mathbf{m},\mathbf{n}',\mathbf{k};t)\right]\right]\\
&+\mathcal{O}(\delta t^2). \qquad (62)
\end{aligned}
$$

bioRxiv preprint doi: https://doi.org/10.1101/041509; this version posted February 26, 2016. The copyright holder for this preprint (which was not certified by peer review) is the author/funder. All rights reserved. No reuse allowed without permission.

If $r_x = 1$

$$\sum_{i=1}^{N_x}\sum_{j=1}^{N_y}\rho_2^{N_x\times N_y}(r_x,0;t+\delta t) =$$

$$\begin{aligned}
&(1-\delta t P_{g_x}N_x - \delta t P_{g_y}N_y)\sum_{i=1}^{N_x}\sum_{j=1}^{N_y}\rho_2^{N_x\times N_y}(r_x,0;t)\\
&+\delta t P_{g_x}\sum_{i=1}^{N_x-1}\sum_{j=1}^{N_y}(r_x-1)\rho_2^{(N_x-1)\times N_y}(r_x-1,0;t)\\
&+\delta t P_{g_x}\sum_{i=1}^{N_x-1}\sum_{j=1}^{N_y}(N_x-1-r_x)\rho_2^{(N_x-1)\times N_y}(r_x,0;t)\\
&+\delta t P_{g_y}\sum_{i=1}^{N_x}\sum_{j=1}^{N_y-1}(N_y-1)\rho_2^{N_x\times(N_y-1)}(r_x,0;t)\\
&+\delta t\frac{P_m}{4}\sum_{i=1}^{N_x}\sum_{j=1}^{N_y}\Bigg[\sum_{\mathbf{k}}^{\mathbf{n}}\left[\rho_3^{N_x\times N_y}(\mathbf{m},\mathbf{n}',\mathbf{k};t)-\rho_3^{N_x\times N_y}(\mathbf{m},\mathbf{n},\mathbf{k}';t)\right]\\
&+\sum_{\mathbf{k}}^{\mathbf{m}}\left[\rho_3^{N_x\times N_y}(\mathbf{m}',\mathbf{n},\mathbf{k};t)-\rho_3^{N_x\times N_y}(\mathbf{m},\mathbf{n},\mathbf{k}';t)\right]\Bigg]\\
&+\delta t\frac{P_p}{4}\sum_{i=1}^{N_x}\sum_{j=1}^{N_y}\Bigg[\sum_{\mathbf{k}\neq\mathbf{n}}^{\mathbf{m}}\left[\rho_3^{N_x\times N_y}(\mathbf{m}',\mathbf{n},\mathbf{k};t)\right]+\rho_2^{N_x\times N_y}(\mathbf{m}',\mathbf{n};t)\\
&+\sum_{\mathbf{k}\neq\mathbf{m}}^{\mathbf{n}}\left[\rho_3^{N_x\times N_y}(\mathbf{m},\mathbf{n}',\mathbf{k};t)\right]+\rho_2^{N_x\times N_y}(\mathbf{m},\mathbf{n}';t)\Bigg]\\
&+\mathcal{O}(\delta t^2).
\end{aligned}\tag{63}$$

From which we can obtain the given equations.